Chromium hazard and risk assessment: New insights from a detailed speciation study in a standard test medium.

Imad Aharchaou, Jean-Sébastien Py, Sébastien Cambier, Jean-Luc Loizeau, Geert Cornelis, Philippe Rousselle, Eric Battaglia, Davide Anselmo Luigi Vignati

CHROMIUM HAZARD AND RISK ASSESSMENT: NEW INSIGHTS FROM A DETAILED SPECIATION STUDY IN A STANDARD TEST MEDIUM

Imad Aharchaou[a], Jean-Sébastien Py[b], Sébastien Cambier[c], Jean-Luc Loizeau[d], Geert Cornelis[e], Philippe Rousselle[a], Eric Battaglia[a], Davide A.L. Vignati[a*]

[a] Laboratoire Interdisciplinaire des Environnements Continentaux UMR 7360, Université de Lorraine and CNRS, Metz, France
[b] Agence nationale de sécurité sanitaire de l'alimentation, de l'environnement et du travail, Laboratoire de Nancy, Nancy, France
[c] Luxembourg Institute of Science and Technology, Esch sur Alzette, Luxembourg
[d] Department F.-A. Forel for Environmental and Aquatic Sciences and Institute for Environmental Sciences, University of Geneva, Genève, Switzerland
[e] Swedish University of Agricultural Sciences, Department of Soil and Environment, Uppsala, Sweden

ABSTRACT

Despite the consensus about the importance of chemical speciation in controlling the bioavailability and ecotoxicity of trace elements, detailed speciation studies during laboratory ecotoxicity testing remain scarce, contributing to uncertainty when extrapolating laboratory findings to real field situations in risk assessment. We characterized the speciation and ecotoxicological effects of Cr^{III} and Cr^{VI} in the OECD medium for algal ecotoxicity testing. Total and dissolved (< 0.22 μm) Cr concentrations showed little variability in media spiked with Cr^{VI}, while dissolved Cr concentration decreased by as much as 80% over 72 hours in medium amended with Cr^{III}. Analyses by ion chromatography ICP-MS highlighted the absence of redox interconversion between Cr^{III} or Cr^{VI} both in the presence and absence of algal cells (*Raphidocelis subcapitata*). Furthermore, the concentration of ionic Cr^{III} dropped below detection limits in less than 2 hours with the corresponding formation of carbonate complexes and Cr hydroxides. Precipitation of Cr^{III} in the form of colloidal particles of variable diameters was confirmed by nanoparticle tracking analysis, spICP-MS and single particle counting. In terms of time weighted dissolved (< 0.22 μm) Cr concentration, Cr^{III} was 4 to 10 times more toxic than Cr^{VI}. However, Cr^{III} ecotoxicity could arise from interactions between free ionic Cr^{III} and algae at the beginning of the test, from the presence of Cr-bearing nanoparticles or a combination of the two. Future ecotoxicological studies must pay more attention to Cr speciation to reliably compare the ecotoxicity of Cr^{III} and Cr^{VI}.

Keywords

Trace metals, Chromium, Metal speciation, Algae, Hazard/Risk assessment

INTRODUCTION

The bioavailability and ecotoxicity of trace elements in natural environments are determined by the complex interplay among the ecological traits of living organisms, the toxicodynamics and toxicokinetics of trace elements, and the elemental speciation in environmental matrices (Fairbrother et al. 2007; Mason 2013; Harris et al. 2014). Elemental speciation refers to various physico-chemical forms in which trace elements occur in a given environment and, in some cases, includes the presence of different oxidation states with contrasting environmental biogeochemistry. In the specific case of chromium, the importance of speciation is well appreciated with regard to its biogeochemical cycle (Masscheleyn et al. 1992; Dominik et al. 2007; Saputro et al. 2014) and biological effects (WHO 2009; WHO 2013). In surface waters, chromium mainly occurs in two oxidation states, namely Cr^{VI} and Cr^{III}, with contrasting environmental and biological behavior. Hexavalent chromium, a recognized human carcinogen, forms negatively charged chemical species, interacts little with colloidal and particulate material, has a high environmental mobility, and easily crosses biological membranes (WHO 2013). In contrast, Cr^{III} preferentially forms positively charged chemical species, tends to associate with colloids or suspended particulate matter and is considered of less ecotoxicological concern (WHO 2009; WHO 2013). In most environmental settings, both redox forms occur simultaneously, albeit in variable proportions (Bobrowski et al. 2004; Saputro et al. 2014) and interconversions between them have been documented along with the corresponding controlling factors (Rai et al. 1989; Richard and Bourg 1991; Lin 2002). However, experimental research on Cr speciation in standardized ecotoxicological test media has received limited attention. Thermodynamic speciation calculations are increasingly used to predict the Cr forms likely to exist in ecotoxicological exposure media, thus aiding experimental planning and data interpretation (Dazy et al. 2008; Didur et al. 2013; Liu et al. 2015). These calculations also suggest that insoluble species of Cr^{III} (mostly Cr oxy-hydroxides) can form in ecotoxicological test media for algae, daphnids and aquatic plants (Dazy et al. 2008; Vignati et al. 2010; Ponti et al. 2014). The presence of such chemical species can modify the fraction of Cr^{III} that is potentially bioavailable for the test organisms during the exposure period, because in most cases it is assumed that the bio-availability of metals is related to the free ion activity (Morel, 1983). Insoluble species also explain the often large differences between total and total filterable (< 0.45 µm) Cr concentrations found in test media spiked with Cr^{III}, the extent depending on medium composition (Chapman et al. 1980; Vignati et al. 2008; Ponti et al. 2014). It should also be noted that filterable (< 0.45 µm) Cr concentrations do not equal the sum of concentrations of truly dissolved Cr species, because the initial formation of precipitates may result in solids having particle sizes below this size cut-off. Furthermore, certain studies present results supporting the conclusion that Cr^{III} is more ecotoxic than Cr^{VI} (Holdway 1988; Thompson et al. 2002; Vignati et al. 2010; Lira-Silva et al. 2011; Kováčik et al. 2015); in contrast with the current consensus considering Cr^{VI} as the most ecotoxic redox form (WHO 2013). A more detailed understanding of Cr speciation in (standardized) laboratory test media used for ecotoxicity testing will help to both reconcile contrasting ecotoxicological results in controlled settings and improve our ability to extrapolate laboratory results to real-field risk assessment situations.

On the basis of the above considerations, three aspects related to Cr speciation, and its changes during a given (standardized) test, appear of particular importance for an improved understanding of the relative ecotoxicity of Cr^{III} and Cr^{VI}: a) the stability of (filterable) Cr concentrations added to the test medium, b) the possibility of redox interconversions between Cr^{III} and Cr^{VI}, and c) the formation of Cr oxyhydroxides (i.e., Cr-bearing nanoparticles). In the present study, the ecotoxicity of three Cr^{III} salts and one Cr^{VI} salt commonly used in ecotoxicological studies was investigated using the standard algal medium ISO 8692 (OECD 2011), hereinafter test medium, as exposure matrix and the green alga *Raphidocelis*

subcapitata as test organism. The behavior and speciation of both Cr^{III} and Cr^{VI} forms, including their possible interconversions, were investigated in detail over 72 h; corresponding to the typical duration of a standard algal test (OECD 2011). Our results showed rapid changes (i.e., within hours) in Cr^{III} speciation which calls for a thorough reconsideration of the current knowledge about the relative ecotoxicity of Cr^{III} and Cr^{VI} in terms of both hazard and risk assessment.

MATERIALS AND METHODS

Chemicals

All chemicals used were of highest purity. For the various experiments, the test medium ISO8692 was prepared as described in OECD guideline 201 (OECD 2011) and spiked with either Cr^{VI} as potassium dichromate ($K_2Cr_2O_7$, VWR, purity 99.8% min, CAS number 7778-50-9) or with one of the following Cr^{III} salts: chromium chloride ($CrCl_3 \cdot 6H_2O$; Alfa Aesar, 99.5% min, Crystalline, CAS number 10060-12-5), chromium potassium sulfate ($KCr(SO_4)_2 \cdot 12H_2O$; VWR, 99%, CAS number 7788-99-0) or chromium nitrate ($Cr(NO_3)_3 \cdot 9H_2O$; Alfa Aesar, 98.5%, Crystalline, CAS number 7789-02-8).
All filtrations were performed using 0.22 µm syringe filters (Millex 33 mm diameter, PVDF, Millipore, reference number SLGV033NB) prewashed one time with 10 mL of diluted (10% v/v) hydrochloric acid (HCl Suprapur 30%, Merck Millipore, lot number Z0309518344) and three times with 10 mL of ultrapure water (Millipore, Q-POD®). A preliminary experiment showed that Millex syringe filters with nominal pore sizes of 0.22 and 0.45 µm yielded comparable results for aliquots of test medium amended with 60 µg Cr^{III}/L (data not shown). All samples for the analysis of total Cr concentration were acidified at 1% v/v with concentrated nitric acid (HNO_3 67%, Prolabo, VWR, batch number 1108110**)**. A solution of 0.4 M nitric acid (Chemlab, suprapur 70%, batch: 221831609) spiked with 1 µg/L of rhodium was used as internal standard during the analyses of Cr speciation.

Chromium ecotoxicity

The ecotoxicity of Cr^{VI} and Cr^{III} salts to the green alga *Raphidocelis subcapitata* (strain 278/4 originally obtained from the Culture Collection of Algae and Protozoa – CCAP – Argyll, Scotland, United Kingdom; formerly known as *Pseudokirchneriella subcapitata*) was evaluated according to OECD guideline 201 (OECD 2011). Tests were performed as previously described (Vignati et al. 2010) using inoculums of 20,000 cells/mL and nominal exposure concentrations of 9, 18, 35, 70, 140, 280, 560, 1125, 2250 µg Cr/L. The effects of Cr salts on algal growth were expressed as the effective exposure concentrations (ECs50) that produced a 50% decrease in algal fluorescence (BMG LabTechnologies, Fluostar), considered as a proxy for algal biomass. The ECs50 were calculated by performing a nonlinear regression on Hill's model with the macro REGTOX (Version EV7.0.4., E. Vindimian) (Vindimian 2010). In the case of Cr^{III}, ECs50 were estimated based on both nominal concentrations and Time-Weighted Mean (TWM) dissolved measured concentrations (OECD 2012). Starting from this point, the terms total and dissolved concentrations will indicate the unfiltered and filtered (0.22 µm) portions of measured Cr levels.

Temporal evolution of Cr concentration in the test medium

Aliquots (50 mL) of freshly prepared test medium were transferred to acid-washed Erlenmeyer flasks (150 mL) and spiked with a Cr concentration corresponding to the ECs50 of either Cr^{III} (added as $CrCl_3 \cdot 6H_2O$) or Cr^{VI} (added as $K_2Cr_2O_7$) in the presence or absence of an initial algal inoculum of 20,000 cells/mL. Aliquots were analyzed for total and dissolved Cr after 0.5, 1, 2, 4, 8, 24, 48, and 72 h of incubation under continuous light (90 – 110 $\mu E/m^2/s$) at 21 ± 2 °C and, for biotic samples only, rotary agitation (100 rpm). For dissolved

Cr determination, the first 5 mL of filtered solution were used for preconditioning the filters and discarded. Preconditioning aimed at removing possible residues of ultrapure water from filter pores and saturate possible sorption sites for Cr. Total and dissolved Cr concentrations were determined by flame atomic absorption spectrometry (FAAS, Perkin-Elmer AAnalyst 100) or, for concentrations < 20 µg/L, graphite furnace atomic absorption spectrometry (GFAAS, Varian spectra 300, using 0.1% $Mg(NO_3)_2$ as matrix modifier according to manufacturer instructions). Quantification limits were 10 µg/L for FAAS and 0.2 µg/L for GFAAS. Certified reference materials SPS-SW1 (2.00 ± 0.02 µg/L) and WW1 (200 ± 1 µg/L), both from SpectraPure standards (Manglerud, Norway), were used as quality controls. All analytical results are expressed in µg Cr/L.

The statistical significance of the temporal changes in Cr concentrations was evaluated by one-way ANOVA with Tukey post-hoc comparison. Visual Minteq modelling (ver 3.1) was done to investigate Cr^{III} speciation in test medium amended with an initial total concentration of 60 µg Cr/L . No redox transformations were assumed, because it will be argued based on experimental proof that these did not occur. Calculations were performed using experimentally measured Cr concentrations and pH values, and the test medium composition as reported in OECD (2011). No modifications were made to the Visual Minteq default database and the Debye-Hückel equation was used for activity corrections.

Chromium redox speciation

To investigate Cr redox speciation and the possible interconversion between Cr^{III} and Cr^{VI}, aliquots (50 mL) of the test medium were spiked with either Cr^{VI} or Cr^{III} (added as chloride) both in absence (abiotic medium) and presence (biotic medium) of algal inoculums (20,000 cells/mL). Nominal Cr concentrations in the spiked solutions were 60 µg/L for Cr^{III} and 115 µg/L for Cr^{VI}, corresponding to the calculated 72 h ECs50 (see section Chromium ecotoxicity in Results and discussion). Samples were analyzed immediately after spiking (t=0) or incubated at 23 ± 1 °C, under continuous light (90 – 110 $\mu E/m^2/s$) and, for biotic samples only, rotary agitation (100 rpm) for 24, 48 and 72 h prior to analysis (Figure S1). At the end of each incubation period, sample aliquots for Cr speciation were filtered as described above. After preconditioning the filters with 5 mL (subsequently discarded) of Cr-amended test medium, 10 mL of filtrate was collected in polystyrene sample vials and immediately analyzed by ion chromatography-inductively coupled plasma mass spectrometry (IC-ICP-MS). Samples were kept at between 4 and 6 °C in a refrigerated sample tray during analysis. An additional abiotic sample of test medium (2 L) was prepared in an acid-washed low-density polyethylene bottle and spiked with 60 µg/L of Cr^{III} to follow more closely the kinetics of the changes in Cr^{III} speciation (Sacher et al. 1999; Séby et al. 2003). Aliquots for analysis were recovered every 20 min over the first 6 hours after spiking and again after 24, 48, and 72 hours of incubation in the same conditions described above.

Trivalent Cr and hexavalent Cr species were separated and quantified by IC-ICP-MS using a Thermo ICS 5000+ pump coupled with an anion exchange column (Thermo AG7 2x50 mm) and connected to the nebulizer of an ICP-MS (Thermo, Series XII) (Table S1). A solution of 0.4 M nitric acid spiked with 1µg/L of rhodium was used to elute the Cr species from the anion exchange column (see Table S1 for more details). The analyses were carried out according to the method developed by the French Agency for Food, Environmental & Occupational Health & Safety (ANSES) on the basis of the application note from the supplier (Sacher et al. 1999; ANSES/LHN/MT-CrVI). Chromium detection was performed at m/z 52 and 53. Experimental IC-ICP-MS results were compared with those of speciation modeling carried out as described previously (section Temporal evolution of Cr concentration) using Visual Minteq.

Formation of Cr nanoparticles in the test medium

Aliquots of test medium were spiked with 60 µg/L of Cr^{III} (added as chloride or nitrate) and the formation of Cr-containing particles was investigated by Nanoparticle Tracking Analysis (NTA), spICP-MS (single particle ICP-MS) and Single Particle Counting (SPC) over 72 h; that is the typical duration of an algal ecotoxicological test. Blank samples consisting of unspiked test medium were systematically analyzed along with the corresponding samples. Total and dissolved Cr concentrations were determined by FAAS during the various experiments.

For NTA (Nanosight NS500; Malvern instruments Ltd, UK), spiked samples were aged for 0, 0.5, 1, 2, 24, 48, and 72 h and assayed (before and after filtration) for particle concentration and particle size distribution (PSD). The NS500 provides detailed analysis of the concentration and size distribution of all types of nanoparticles from 10 nm to 1000 nm in diameter (Carr and Wright 2013) using the properties of both light scattering and Brownian motion in liquid suspensions. Particles in suspension in the sample chamber (volume = 0.3 mL) were visualized using a 20x magnification microscope equipped with a camera operated at 25 frames per second for 60 s. The resulting video files were elaborated using the built-in software (NTA 2.3 build 0033) to calculate the hydrodynamic diameter of the individually tracked particles. After each measurement, the sample chamber was flushed with milliQ water and reloaded with the next sample aliquot. All measurements were done in triplicate and the mean (± one standard deviation) of particle concentration and average size calculated (see supplementary information for protocol optimization).

While NTA determines the total particle count, spICP-MS (Perkin Elmer NexION 350D ICP-MS) was used to specifically measure Cr-containing particles. Samples were aged for 0, 24, 48 and 72 h and diluted to a theoretical concentration of 0.06 µg/L total Cr before analysis. The transport efficiency was calculated based on a dissolved standard curve of Au stabilized by 0.1 % cysteine and on the TEM-based median size (56 nm) of gold nanoparticles (NIST8013, nominal diameter 60 nm) using the method of Pace et al. (2011). Data acquisition was performed in fast acquisition scanning technique (FAST) mode with a dwell time of 50 µs over 100 s. Raw data (two million readings per sample) were extracted and loaded into the Nanocount software (http://blogg.slu.se/nanocount/) for the determination of particle number and particle size distribution. Correction for dissolved concentrations was performed using outlier analysis based on a $5 \times \sigma$ criterion specifically developed for FAST data (Tuoriniemi et al. 2015). Peak integration time was set to 20 ms and the minimum detectable cluster was set at 4 ions. Distributions of the corresponding spherical size were calculated assuming a $Cr(OH)_3$ ($\rho = 3.11$ g/cm^3) composition and a spherical shape. It should be noted that these were assumptions as the exact composition and shape of the formed particles are unknown. However, considering the measured pH range of the test medium initially spiked with 60 µg Cr/L (7.8–7.9 units), trivalent chromium is expected to rapidly undergo hydrolysis and form amorphous oxyhydroxides (Rai et al. 1989; Kotaś and Stasicka 2000). The assumption on particle shape would allow comparison with the results obtained using other methods.

To detect the presence of particles outside the NTA and spICP-MS measuring range, samples were analyzed after 0, 24, 48, and 72 hours of incubation using three Single Particle Counters (SPCs): a high sensitivity in-situ monitor (HSLIS) Model M50 for the range 50 to 200 nm and two Volumetric Spectrometers (LiQuilaz-S02 and LiQuilaz-S05, Particle Measuring Systems, Boulder, CO, U.S.A) for the ranges 200 to 2000 nm and 500 nm to 20 µm, respectively. The SPCs use light scattering to count individual particles across 31 size classes with some overlapping between the LiQuilaz-S02 and S05 (Rossé and Loizeau 2003). Results for spiked medium were corrected for blank values.

RESULTS AND DISCUSSION

Chromium ecotoxicity and temporal evolution of Cr concentrations

Results of ecotoxicity tests were highly reproducible with ECs50 at 72 h (mean value ± one standard deviation) of 113 ± 3 µg/L (n = 3) for $K_2Cr_2O_7$, 59 ± 3 µg/L for $CrCl_3 \cdot 6H_2O$ (n = 6), 61 ± 8 µg/L for $Cr(NO_3)_3 \cdot 9H_2O$ (n = 3) and 62 ± 3 µg/L for $KCr(SO_4)_2 \cdot 12H_2O$ (n=3). The ECs50 values reported in the literature for freshwater algae range from 130 to 470 µg/L for Cr^{VI} and from 30 µg/L to over 1000 µg/L for Cr^{III} (WHO 2009; Vignati et al. 2010; OECD 2011; WHO 2013). In the case of Cr^{VI}, a ring test involving 16 laboratories determined a range of 72h-ECs50 between 70 and 260 µg Cr/L for *Scenedesmus subspicatus* and *Selenastrum capricornutum* (a former name for *R. subcapitata*) based on algal biomass endpoint (Munn et al. 2005; WHO 2013); which agrees with our results. In the case of Cr^{III}, our results are in the low range of the values reported in the literature and indicate a higher toxicity of Cr^{III} compared with Cr^{VI}; an occurrence also reported in previous research (Holdway 1988; Thompson et al. 2002; Vignati et al. 2010; Lira-Silva et al. 2011; Kováčik et al. 2015). Further insights in the relative ecotoxicity of the two redox forms of Cr can be gained by examining their behavior in the test medium. In particular, the detailed examination of Cr^{VI} and Cr^{III} behavior added to the test medium at concentrations corresponding to their respective ECs50 allows to exactly determine the actual concentrations responsible for the observed effects.

At t = 0 h, the measured total and dissolved Cr concentrations (added as Cr^{III}) were similar and corresponded to the expected nominal values in both abiotic and biotic media. In the absence of algae, total Cr concentrations remained within 20% of the initial value over the first 24 hours and had decreased by about 40% after 72 h. In the same experiment, dissolved Cr concentrations remained within 20% of the initial values only over the first two hours, but had dropped by 40% eight hours after spiking and by 83% after 72 h (Figure 1). The decrease in total Cr concentrations indicates that some of the added Cr may be lost to the walls of the test vessel over time. However, comparison of total and dissolved concentrations indicates that ca. 50% of the added Cr likely occurs in the form of colloidal or particulate form (most likely amorphous Cr oxyhydroxides) starting from 24 hours after spiking (i.e., for over 2/3 of the test duration). Calculations in Visual Minteq for an initial concentration of 60 µg/L as Cr^{III} predicted that, in the observed pH range of 7.8 to 7.9, the $Cr(OH)_3$ species should account for 92–94 % of the total Cr. Furthermore, about 80% of the initially added Cr^{III} was predicted to precipitate in the form of amorphous $Cr(OH)_3$, in very good agreement with the 80% decrease of the corresponding dissolved Cr concentration over 72h (Figure 1). Colloid/nanoparticle formation was indeed confirmed using NTA and spICP-MS (see section Formation of Cr nanoparticles in Results and Discussion). Analogous calculations using the dissolved Cr concentration measured at 72h (11±0.25 µg/Cr L, n=3) also predicted that $Cr(OH)_3$ would account for over 90% of the measured Cr concentration, but with less than 2% occurring in the precipitated phase. In both cases, the sum of the positively charged species $Cr(OH)_2^+$ and $CrOH^{2+}$ was predicted to represent about 3.5% of the total dissolved Cr and EDTA complexes were about 2.5%. Further comparison between speciation calculations and analytical results is presented in the next section.

The difference between total and dissolved Cr concentrations becomes statistically significant starting from 8 h after spiking (one-way Anova with Tukey post-hoc comparison, $p < 0.01$). Considering the temporal decrease of the dissolved Cr concentration, assumed as a better proxy of the Cr potentially available to the algae (see de Paiva Magalhães et al. 2015 and references therein for a detailed discussion), the time-weighed mean (TMW) (OECD 2012) exposure concentration of the algae to Cr (added as Cr^{III}) was about 25 µg/L for an initial addition of 60 µg/L as Cr^{III}. Similar behavior of total and dissolved Cr concentration was observed over the concentration range 20 – 7,000 µg/L for $CrCl_3$ and for selected

concentrations of $Cr(NO_3)_3$ and $CrKSO_4$ (Figures S2–S4); confirming that the decrease in the dissolved exposure concentrations must be considered and quantified when testing Cr^{III} toxicity in standardized laboratory media. These observations corroborate previous findings obtained by measuring the decrease in Cr concentrations in test medium directly in 96-well microplates in the absence of algae and without actually providing information on the total vs. dissolved Cr concentrations (Vignati et al. 2008; Vignati et al. 2010).

In the presence of algae, both total and dissolved Cr concentrations decreased with time (Figure 1) and the decrease was more marked for the dissolved concentrations (over 95% after 72 hours). The incomplete recovery of total Cr was likely caused by attachment of algal cells to the vessel's walls despite the constant agitation. Most importantly, the differences between dissolved Cr concentrations in the absence and presence of algae became statistically significant starting from 24 h after spiking (one-way Anova with Tukey post-hoc comparison, $p < 0.01$), indicating adsorption onto or absorption into the algal cells of most of the available dissolved Cr. Based on the dissolved Cr concentrations in the presence of algae, the 72 h TMW effect concentration (EC50) for algal growth (in terms of biomass) was 11.5 µg/L. Analogous experiments performed with aliquots of test medium amended with Cr^{VI} at the corresponding EC50 concentration (115 µg/L) did not show significant changes in total or dissolved Cr concentration neither in the absence nor in the presence of algae (Figure S5). The above observations lead us to the conclusion that Cr^{III} is 4 to 10 times more toxic than Cr^{VI} when the 72 h EC50 for Cr^{III} is expressed as the TWM dissolved concentration estimated from measurements in the absence or presence of algae, respectively. However, the presence of algae had no measurable effect on dissolved Cr^{VI} concentrations (Figure S6). One possibility is that the entrance of minimal quantities of Cr^{VI} into the cells may suffice to reduce algal biomass, which would support the current consensus that Cr^{VI} is more toxic than Cr^{III}. On the other hand, exposure to Cr^{VI} has been shown to cause lysis of *R. subcapitata* cells at concentrations of 1.75 mg/L or higher added to an algal inoculum of 2×10^5 cells/mL (Labra et al. 2007); which corresponds to an initial quantity of 8.75 ng of Cr^{VI} per algal cell at the beginning of the experiment (our calculation). This figure compares favorably with the value of 5.75 ng of Cr^{VI} per algal cell in our experimental conditions for an initial spike of 115 µg/L. Upon cell lysis, the initially internalized Cr^{VI} would be released back to the test medium resulting in an apparent stable total (dissolved) Cr concentration over the duration of the experiment. Note that Cr^{VI} can undergo intracellular reduction to Cr^{III} (Cheung and Gu 2007; Volland et al. 2012; Kováčik et al. 2015) which could also be released back to the test medium upon cell lysis; possibly in association with intracellular constituents preventing its precipitation in the test medium. While no experiments were performed to determine if cell lysis had occurred, we verified possible changes in the redox state of Cr in the test medium over the exposure duration.

Chromium redox speciation

Aliquots of test medium spiked with Cr^{VI} exhibited a single peak, corresponding to the one observed in a standard solution of Cr^{VI}, with a retention time of about 50 s regardless of the presence of algae and of the incubation time (Figures 2A and S6). The total Cr^{VI} concentration, determined from total peak area, was 118 µg/L at t=0 and 120 µg/L after 72h of incubation in the abiotic test medium and 137 µg/L at t=0 and 120 µg/L after 72h in the biotic medium. No peaks corresponding to Cr^{III} were observed in either abiotic or biotic test medium (Figures 2A and S6). While this result does not provide information on possible Cr^{VI} to Cr^{III} interconversion in the intracellular environment (Shanker et al. 2005; Viti et al. 2014; Kováčik et al. 2015), it shows that algal cells are exposed to a practically constant concentration of Cr^{VI} throughout the test duration. The corresponding ECs50 values for Cr^{VI}

can therefore be confidently ascribed to this specific redox form and calculated from the concentrations initially added to the test medium.

On the other hand, marked and rapid changes in Cr speciation occurred in medium aliquots amended with Cr^{III}. At t=0 and in the absence of algae, a single peak at a retention time of about 100 s, corresponding to the hydrated Cr^{III} ion, was observed (Figure 2B). The corresponding dissolved Cr^{III} concentration determined by IC-ICP-MS was 57 µg/L, in agreement with the expected value of 60 µg/L. However, after 24 h of incubation, the peak area at 100 s had dropped by 99% and the corresponding dissolved Cr^{III} concentration at 72 h was only 0.39 µg/L (Figure 2B). Starting from 24 h after spiking, two additional peaks were observed at retention times around 45 s and 75 s (Figure 2B). Considering the measured pH range of the test medium (7.5–7.9 for medium aliquouts amended with Cr^{III} concentrations between 20 and 1250 µg Cr/L), Cr^{III} is expected to rapidly undergo hydrolysis (Rai et al. 1989; Richard and Bourg 1991; Kotaś and Stasicka 2000) and the peaks at 45 and 75 s likely correspond to the hydrolytic Cr^{III} complexes $Cr(OH)^{2+}$ and $Cr(OH)_3^0$ (Séby et al. 2003).Addition of 5 µg/L of Cr^{VI} to an aliquot of the solution initially spiked with 60 µg/L of Cr^{III} and aged for 4 h resulted in the expected Cr^{VI} peak at 50 s, thus confirming that the peak at 45 s was not the results of an oxidation of Cr^{III} to Cr^{VI} during the experiment (Figures 2C and S6).

As already seen in the previous section, for an initial concentration of 60 µg/L of Cr^{III}, speciation calculations using Visual Minteq suggest that, at equilibrium, the positively charged species $Cr(OH)_2^+$ and $CrOH^{2+}$ should represent about 3.5% of the total in the observed pH range of 7.8–7.9. Assuming a dissolved Cr concentration of 11 µg Cr/L after 72h of incubation (see previous section and figure 1), the theoretical concentration of positively charged Cr species at the end of the exposure period would be 0.2–0.4 µg/L; in agreement with the IC-ICP-MS speciation results (Figure 2B).

Samples spiked with Cr^{III} in the presence of algae showed the three distinct peaks at retention times of about 100 s, 75 s, and 45 s already at t = 0 (Figure S6). The area of all peaks rapidly decreased and became practically negligible after 24 hours of incubation (Figure S6). In the presence of algae, the concentration of hydrated Cr^{III} (peak at 100 s) decreased from 30 µg/L at t = 0 to 0.14 µg/L at t = 72 h (Figure S6). The discrepancy between the measured (30 µg/L) and expected concentration (60 µg/L) at t = 0 can be explained by a more rapid formation of hydrolysis products. Indeed, the presence of particular microenvironments with increased pH around algal cells and colonies was reported to enhance Fe hydrolysis (Sunda and Huntsman 2003) and an analogous phenomenon may occur in the case of Cr^{III}. Again, no peak indicative of the formation of Cr^{VI} was identified throughout the experiment duration so that the ecotoxicological effects discussed previously (section Chromium ecotoxicity in Results and Discussion) can be ascribed to Cr^{III}.

The disappearance of the chromatographic peak of hydrated Cr^{III} (t = 100 s) between 0 and 24 h of incubation prompted us to examine the changes in Cr^{III} speciation at shorter time intervals. Note that, given the absence of calibration standards for the peaks at 45 and 75 s, the changes in the relative importance of the chromatographic peaks can be discussed solely on the basis of their signal intensities. Immediately after spiking, 84% of dissolved Cr was present as hydrated Cr^{III} (retention time 100 s) with the peaks at 75 s and 45 s representing about 8% of the total signal each (Figures 2C and 3). The peak of hydrated ionic Cr^{III} at 100 s decreased very rapidly and was only 2% of the initial dissolved Cr concentration after 6 hours of incubation (Figure 3). At the same time, the peak at 75s increased up to 56% of the total signal 1 hour after spiking and then slowly decreased to 40% after 6 h. The peak at 45 s accounted for 7 and 10% of the total signal regardless of the incubation time (Figure 3). Both the sum of the signals of the three peaks and the corresponding dissolved Cr signal (assayed

by ICP-MS) decreased by 50% and 40% compared with their respective initial values (Figure 3).

Samples collected after 24, 48, and 72 h of incubation confirmed the initial decreasing trend and, in the case of dissolved Cr, were comparable with the results obtained by FAAS (Figure 1). The difference between dissolved Cr (ICP-MS) and the sum of various Cr peaks (IC-ICP-MS) may be due to nanoparticle formation depositing in the column and going undetected. On the other hand, the signal of total Cr (in terms of relative intensity measured by ICP-MS) remained within 20% of the initial value (Figure 3). Overall, the rapid changes in Cr^{III} speciation added to the test medium (particularly the disappearance of ionic Cr^{III} in less than 2 h) arise the question of which Cr^{III} species are actually responsible for the observed decrease in algal biomass during ecotoxicity testing. These considerations will be developed later in the text (section Implications for Cr hazard and risk assessment) after the presentation of the results confirming the formation of Cr-bearing particles in the test medium.

Formation of chromium (nano)particles

NTA analysis showed that colloidal particles formed within minutes after adding soluble Cr^{III} into the test medium. Particle concentration and size ranged between 9.64×10^8 and 29.7×10^8 particles/mL and 80 and 140 nm, respectively (Figure 4). The particle concentration was $0.17 \pm 0.10 \times 10^8$ particles/mL in test medium without added Cr^{III} (Figure 4). Filtration (0.22 µm) of Cr^{III}-amended aliquots of test medium lowered particle concentration to around 0.6×10^8 particles/mL, but did not decrease their size by more than 25% (Figure 4). Total Cr concentration remained within ± 20% of initial value over the entire experiment duration. Dissolved Cr concentrations also did not change during the first 2 h of incubation, but then progressively decreased to 26% of the initial value after 72h (Figure 4). The concomitant removal of particles and decrease in dissolved Cr concentration (Figure 4) confirms the formation of Cr containing (nano)particles starting from initially soluble Cr^{III} salts for incubation times > 24 h (Figure 4). The experimental decrease of dissolved Cr concentrations is in agreement with the theoretical calculation performed with Visual Minteq (see Chromium ecotoxicity in Results and discussion).

Analysis by spICP-MS confirmed that the nanoparticles formed immediately after spiking actually contained Cr (Figure S11). The orders of magnitude of size is similar to those measured using NTA (Figure S11 and Figure 4), at least when using the assumed composition and shape (Table S3). On the other hand, spICP-MS detected an increase in particle number from 5×10^6 ($t \leq 24$ h) to 2×10^8 ($t \geq 72$ h), suggesting that the mass percentage of Cr^{III} occurring as particles increased from 4% at 0 h to 20% at 72 h to 76% at 96 h. Differences in particle numbers estimated by spICP-MS and NTA likely arise from the specific technical features of the two methods. Large particles do not manage to pass a spray chamber and are therefore not measured during spICP-MS (Tuoriniemi et al. 2017), which therefore tends to favor small particles as long as they are larger than the detection limit of approx. 90 nm. NTA, in contrast, preferentially detects relatively large particles that scatter more light and is less accurate in detecting relatively small particles. Note also that the particle size distributions detected with spICP-MS abruptly stop at the size detection limit. Thus, despite the two techniques yielding similar average particle sizes, NTA likely observes a fairly constant number concentration of relatively large particles that are mostly removed by filtration, while spICPMS observes an increase in the number of (relatively small) particles with time (Figure 4 and S11). At short incubation times, a very large mass of Cr may reside in the particle fraction that can pass a 0.22 µm filter without being detected by neither NTA nor spICP-MS. Hence, a decrease Cr mass concentration is not observed when filtering samples at 0.22 µm at short incubation times (Figure 4). Measurement of total and dissolved Fe (data not shown) allowed to exclude the formation of Fe-bearing particles (including mixed Cr-

Fe(oxy)hydroxides) (Sass and Rai 1987) and thus the possibility of indirect ecotoxic effect of Cr^{III} via sequestration of the essential nutrient Fe. Interestingly, model calculations with Visual Minteq predicted that the test medium should be oversaturated with respect to different mineral phases including several Fe-containing minerals and hydroxyapatite. The exact chemical nature of particles formed in Cr-spiked test medium clearly deserves further experimental investigation, especially at short incubation times for which the assumption of equilibrium is unlikely to be valid. Finally, removal of particles with sizes between 80 and 140 nm by filters with a 0.22 µm nominal cut-off can be explained by an actual smaller cut-off of the filters' pores (She et al. 2008) or by the formation of larger particles undetectable via NTA and spICP-MS.

Measurements by SPC confirmed the presence of particles in the same range identified by NTA and spICP-MS, but also of particles larger than 300 nm in unfiltered test medium spiked with Cr^{III} and incubated for 24, 48, and 72 hours (Figure 5 and S7). At t=0, only particles between 50 and 150 nm were observed at a concentration of 3.2×10^5 particles/mL. After 24 hours, the concentration of particles between 50 and 200 nm increased to 6.1×10^6 particles/mL and particles larger than 300 nm (8.5×10^3 particles/mL) had also appeared. Particles in the range 50–200 nm were still present after 48 (6.5×10^6 particles/mL) and 72 h (9.8×10^6 particles/mL) of incubation, while particles larger than 300 nm eventually disappeared after 72 h (Figure 5). The latter observation suggests the formation of particles too large to be measured by the instruments or, more likely, settling too quickly to be effectively sampled by the instrument.

Based on the analysis of total and dissolved Cr in the samples subject to SPC measurements (figure S7), 45 µg of Cr (75% of the Cr^{III} initially added to the test medium) had been incorporated in the observed particles after 72 hours. This result agrees well with the corresponding Visual Minteq calculations (see section Cr ecotoxicity in Results and discussion for details). Assuming a density of 3.11 g/cm^3 for the amorphous Cr oxyhydroxides likely occurring in the medium, the total volume of the particles would be approx. 1.45×10^{-14} m^3/mL. Given an approximate volume of 5.24×10^{-22} m^3 for an individual (spherical) particle with a diameter of 100 nm, a mass of Cr of 45 µg would be enough to form 2.76×10^7 particles/mL. The presence of larger particles, unaccounted for in the previous calculation, can be invoked to explain the difference between calculations and SPC measurements.

Implications for Cr hazard and risk assessment

Our results show that Cr^{III} speciation into a standardized ecotoxicological test medium for algae changes within a few hours after spiking; even when the total Cr^{III} concentration remains comparatively stable. Similar, although less detailed, investigations on daphnids (Ponti et al. 2014) and bacteria (Bencheikh-Latmani et al. 2007) suggest that such behavior may be common in ecotoxicological media whose composition favors the formation of Cr^{III} hydroxides. Thus, new ecotoxicological data for the hazard assessment of Cr^{III} must be obtained by considering the recommendations originally developed for sparingly soluble substances (ISO 14442 2006) [46]. In particular, in the case of marked differences (> 20%) between nominal and actual concentration, the corresponding EC50 for Cr^{III} must be calculated as the TWM of the dissolved concentration (OECD 2012). The excellent agreement between experimental results and thermodynamic modeling of speciation equally suggests that our observations could have a broader validity, although the kinetics of temporal speciation changes may vary across media and as a function of initial Cr^{III} concentration. Furthermore, following our IC-ICPMS results, the question of the actual Cr^{III} species responsible for the observed ecotoxicological effects in living organisms deserves additional study. An application of the biotic ligand model to the study of root elongation in barley

(Song et al. 2014) suggested Cr^{3+} and $Cr(OH)^{2+}$ as the two biologically active chemical species in controlling the effects of Cr^{III}. However, the rapid disappearance (< 2 h) of ionic Cr from the test medium questions the role of such species in determining the observed algal response. One possibility is that a pulse exposure to 60 µg/L of truly dissolved Cr^{III} at the beginning of the test can cause a 50% reduction in algal biomass after incubation over 72 h. Alternatively, the residual concentration of ionic Cr^{III} after 2 h (less than 1 µg/L) determines the effect observed at the end of the test or the other Cr^{III} species also contribute to the observed toxicity. The formation of some Cr-bearing (nano)particles over the course of the test also points to a possible nano-ecotoxicological dimension in the toxicity of Cr^{III} to algae. In particular, freshly formed $Cr(OH)_3$ particles can lead to the formation of "transiently available Cr^{III} species" which may be highly toxic (Bencheikh-Latmani et al. 2007). The existence of monomeric and polymeric Cr^{III} being documented in environmental samples (Hu et al. 2016), both Cr hydroxides and Cr-bearing (nano)particles may have an ecotoxicological role outside laboratory settings and deserve consideration in risk assessment for Cr^{III}.
The present study does not question the high ecotoxicity of Cr^{VI}, but it adds to the growing evidence that the biological effects of Cr^{III} strongly depend on the composition of the medium used for testing and are likely underestimated (Lira-Silva et al. 2011; Ponti et al. 2014). In this context, the paradigm 'Cr^{VI} is more toxic than Cr^{III},' increasingly appears as an oversimplified representation of environmental reality. In this context, more detailed studies on the speciation Cr^{III} in standardized ecotoxicological laboratory settings are highly desirable for at least three reasons. First, reduction of Cr^{VI} to Cr^{III} is a typical strategy for remediation of Cr-contaminated matrices and environments; second Cr contamination remains a serious environmental problem in several low to middle income countries whose economic activity is linked with the material demands of the current lifestyle in developed countries (Pure Earth and Green Cross 2016); third the safe perspective use of Cr_2O_3 nanoparticles is linked to their intrinsic properties, but also to the possible release of soluble Cr in either redox forms (Horie et al. 2013; da Costa et al. 2016; Puerari et al. 2016). In all cases, the appropriate knowledge of the actual ecotoxicity of Cr^{VI} and Cr^{III} necessary to assess the environmental risks of Cr appears incomplete. Identifying the exact chemical species responsible for ecotoxicological effects, especially in the case of Cr^{III}, will facilitate extrapolation of laboratory findings to complex environmental realities and the associated remediation/management decision.

Supplemental data— The Supplemental Data are available on the Wiley Online Library at DOI: 10.1002/etc.xxx. Details for IC-ICP-MS experiments and analytical procedures, temporal evolution of dissolved Cr^{III} and Cr^{VI} concentrations, complementary IC-ICP-MS results, optimization and details of NTA and spICP-MS procedures and additional measurements of particle size distribution and number by SPC, NTA and spICP-MS.

Acknowledgment
This work is part of the PhD thesis of I. Aharchaou who is supported by the French Ministry of Education. The financial support of the CNRS (project EC2CO Insokintox) is greatly acknowledged. We thank A. Garnier (LHN, ANSES, Nancy) for help with IC-ICP-MS analysis. The contributions of S. Cambier were in part made possible within NANION (FNR/12/SR/4009651-Fonds National de la Recherche Luxembourg). We are grateful to E. Szalinska (AGH University of Science and Technology, Krakow, Poland) for her help in some experiments. D. Vignati and G. Cornelis acknowledge the support of COST action ES1205 (STSM 35421).

REFERENCES

Anses. Méthode d'analyse du chrome hexavalent dans les eaux. [accessed 2016 Apr 11]. https://www.anses.fr/fr/system/files/MethodeChromeHexavalentEaux-Consultation.pdf.

Bencheikh-Latmani R, Obraztsova A, Mackey MR, Ellisman MH, Tebo BM. 2007. Toxicity of Cr(III) to *Shewanella sp*. Strain MR-4 during Cr(VI) Reduction. Environ. Sci. Technol. 41:214–220. doi:10.1021/es0622655.

Bobrowski A, Baś B, Dominik J, Niewiara E, Szalińska E, Vignati D, Zarbski J. 2004. Chromium speciation study in polluted waters using catalytic adsorptive stripping voltammetry and tangential flow filtration. Talanta 63:1003–1012. doi:10.1016/j.talanta.2004.01.004.

Carr , B, Wright, M. 2013. Nanoparticle Tracking Analysis. [accessed 2016 Mar 21]. http://particularsciences.ie/psl/brochures/supplier_brochures_pdf/nta_brochure.pdf.

Chapman GA, Ota S, Recht F, Corvallis Environmental Research Laboratory. 1980. Effects of water hardness on the toxicity of metals to Daphnia magna: status report - January 1980. Corvallis, Ore.: U.S. Environmental Protection Agency, Corvallis Environmental Research Laboratory.

Cheung KH, Gu J-D. 2007. Mechanism of hexavalent chromium detoxification by microorganisms and bioremediation application potential: A review. Int. Biodeterior. Biodegrad. 59:8–15. doi:10.1016/j.ibiod.2006.05.002.

da Costa CH da, Perreault F, Oukarroum A, Melegari SP, Popovic R, Matias WG. 2016. Effect of chromium oxide (III) nanoparticles on the production of reactive oxygen species and photosystem II activity in the green alga *Chlamydomonas reinhardtii*. Sci. Total Environ. 565:951–960. doi:10.1016/j.scitotenv.2016.01.028.

Dazy M, Béraud E, Cotelle S, Meux E, Masfaraud J-F, Férard J-F. 2008. Antioxidant enzyme activities as affected by trivalent and hexavalent chromium species in *Fontinalis antipyretica* Hedw. Chemosphere 73:281–290. doi:10.1016/j.chemosphere.2008.06.044.

de Paiva Magalhães D, da Costa Marques MR, Baptista DF, Buss DF. 2015. Metal bioavailability and toxicity in freshwaters. Environmental Chemistry Letters 13:69–87.

Didur O, Dewez D, Popovic R. 2013. Alteration of chromium effect on photosystem II activity in *Chlamydomonas reinhardtii* cultures under different synchronized state of the cell cycle. Environ. Sci. Pollut. Res. 20:1870–1875. doi:10.1007/s11356-012-1389-8.

Dominik J, Vignati D a. L, Koukal B, Pereira de Abreu M-H, Kottelat R, Szalinska E, Baś B, Bobrowski A. 2007. Speciation and Environmental Fate of Chromium in Rivers Contaminated with Tannery Effluents. Eng. Life Sci. 7:155–169. doi:10.1002/elsc.200620182.

Vindimian.E. 2010. REGTOX: macro Excel™ for dose-response modelling.

Fairbrother A, Wenstel R, Sappington K, Wood W. 2007. Framework for Metals Risk Assessment. Ecotoxicol. Environ. Saf. 68:145–227. doi:10.1016/j.ecoenv.2007.03.015.

Harris CA, Scott AP, Johnson AC, Panter GH, Sheahan D, Roberts M, Sumpter JP. 2014. Principles of Sound Ecotoxicology. Environ. Sci. Technol. 48:3100–3111. doi:10.1021/es4047507.

Holdway D. 1988. The toxicity of chromium to fish. In Nriagu JO, Nieboer E, eds, Chromium in the natural and human environments. John Wiley & Sons, pp. 369–397.

Horie M, Nishio K, Endoh S, Kato H, Fujita K, Miyauchi A, Nakamura A, Kinugasa S, Yamamoto K, Niki E, et al. 2013. Chromium(III) oxide nanoparticles induced remarkable oxidative stress and apoptosis on culture cells. Environ. Toxicol. 28:61–75. doi:10.1002/tox.20695.

Hu L, Cai Y, Jiang G. 2016. Occurrence and speciation of polymeric chromium(III), monomeric chromium(III) and chromium(VI) in environmental samples. Chemosphere 156:14–20. doi:10.1016/j.chemosphere.2016.04.100.

Munn S. J Allanou, R Aschberger, K Berthault, F Cosgrove, O Luotamo, M Vegro. 2005. Chromium trioxide, sodium chromate, sodium dichromate, ammonium dichromate, potassium dichromate, EUR 21508 EN. *European Union Risk Assessment Report*, *53*..

ISO 14442. 2006. Water quality -- Guidelines for algal growth inhibition tests with poorly soluble materials, volatile compounds, metals and waste water.

Kotaś J, Stasicka Z. 2000. Chromium occurrence in the environment and methods of its speciation. Environ. Pollut. 107:263–283. doi:10.1016/S0269-7491(99)00168-2.

Kováčik J, Babula P, Hedbavny J, Kryštofová O, Provaznik I. 2015. Physiology and methodology of chromium toxicity using alga *Scenedesmus quadricauda* as model object. Chemosphere 120:23–30. doi:10.1016/j.chemosphere.2014.05.074.

Labra M, Bernasconi M, Grassi F, De Mattia F, Sgorbati S, Airoldi R, Citterio S. 2007. Toxic and genotoxic effects of potassium dichromate in *Pseudokirchneriella subcapitata* detected by microscopy and AFLP marker analysis. Aquat. Bot. 86:229–235. doi:10.1016/j.aquabot.2006.10.006.

Lin C-J. 2002. The Chemical Transformations of Chromium in Natural Waters – A Model Study. Water. Air. Soil Pollut. 139:137–158. doi:10.1023/A:1015870907389.

Lira-Silva E, Ramírez-Lima IS, Olín-Sandoval V, García-García JD, García-Contreras R, Moreno-Sánchez R, Jasso-Chávez R. 2011. Removal, accumulation and resistance to chromium in heterotrophic *Euglena gracilis*. J. Hazard. Mater. 193:216–224. doi:10.1016/j.jhazmat.2011.07.056.

Liu J, Fu J, Ning X 'an, Sun S, Wang Y, Xie W, Huang S, Zhong S. 2015. An experimental and thermodynamic equilibrium investigation of the Pb, Zn, Cr, Cu, Mn and Ni partitioning during sewage sludge incineration. J. Environ. Sci. 35:43–54. doi:10.1016/j.jes.2015.01.027.

Mason RP. 2013. Trace Metals in Aquatic Systems. John Wiley & Sons.

Masscheleyn PH, Pardue JH, DeLaune RD, Patrick J WH. 1992. Chromium Redox Chemistry in a Lower Mississippi Valley Bottomland Hardwood Wetland. Environ. Sci. Technol. 26:1217–1226. doi:10.1021/es50002a611.

Morel, F.M.M. 1983. Principles of Aquatic Chemistry. Wiley, New York.

OECD. 2011. Test No. 201: Freshwater Alga and Cyanobacteria, Growth Inhibition Test. Paris: Organisation for Economic Co-operation and Development. [accessed 2015 Sep 18]. http://www.oecd-ilibrary.org/content/book/9789264069923-en.

OECD. 2012. Test No. 211: Daphnia magna Reproduction Test. Paris: Organisation for Economic Co-operation and Development. [accessed 2015 Sep 18]. http://www.oecd-ilibrary.org/content/book/9789264185203-en.

World Health Organization. 2009. Inorganic Chromium(III) Compounds.

World Health Organization. 2013. Inorganic Chromium(VI) Compounds.

Pace HE, Rogers NJ, Jarolimek C, Coleman VA, Higgins CP, Ranville JF. 2011. Determining Transport Efficiency for the Purpose of Counting and Sizing Nanoparticles via Single Particle Inductively Coupled Plasma Mass Spectrometry. Anal. Chem. 83:9361–9369. doi:10.1021/ac201952t.

Ponti B, Bettinetti R, Dossi C, Vignati DAL. 2014. How reliable are data for the ecotoxicity of trivalent chromium to *Daphnia magna*? Environ. Toxicol. Chem. 33:2280–2287. doi:10.1002/etc.2672.

Puerari RC, da Costa CH, Vicentini DS, Fuzinatto CF, Melegari SP, Schmidt ÉC, Bouzon ZL, Matias WG. 2016. Synthesis, characterization and toxicological evaluation of Cr2O3 nanoparticles using *Daphnia magna* and *Aliivibrio fischeri*. Ecotoxicol. Environ. Saf. 128:36–43. doi:10.1016/j.ecoenv.2016.02.011.

Pure Earth, Green Cross. 2016. The World's Worst Pollution Problems 2016: The Toxics Beneath Our Feet. [accessed 2016 Nov 19].

Rai D, Eary LE, Zachara JM. 1989. Environmental chemistry of chromium. Sci. Total Environ. 86:15–23. doi:10.1016/0048-9697(89)90189-7.

Richard FC, Bourg ACM. 1991. Aqueous geochemistry of chromium: A review. Water Res. 25:807–816. doi:10.1016/0043-1354(91)90160-R.

Rossé P, Loizeau J-L. 2003. Use of single particle counters for the determination of the number and size distribution of colloids in natural surface waters. Colloids Surf. Physicochem. Eng. Asp. 217:109–120. doi:10.1016/S0927-7757(02)00565-4.

Sacher F, Raue B, Klinger J, Brauch H-J. 1999. Simultaneous Determination of Cr(III) and Cr(VI) in Ground and Drinking Waters by IC-ICP-MS. Int. J. Environ. Anal. Chem. 74:191–201. doi:10.1080/03067319908031425.

Saputro S, Yoshimura K, Matsuoka S, Takehara K, Narsito, Aizawa J, Tennichi Y. 2014. Speciation of dissolved chromium and the mechanisms controlling its concentration in natural water. Chem. Geol. 364:33–41. doi:10.1016/j.chemgeo.2013.11.024.

Sass BM, Rai D. 1987. Solubility of amorphous chromium(III)-iron(III) hydroxide solid solutions. Inorg. Chem. 26:2228–2232. doi:10.1021/ic00261a013.

Séby F, Charles S, Gagean M, Garraud H, Donard OFX. 2003. Chromium speciation by hyphenation of high-performance liquid chromatography to inductively coupled plasma-mass spectrometry—study of the influence of interfering ions. J. Anal. At. Spectrom. 18:1386–1390. doi:10.1039/B306249J.

Shanker AK, Cervantes C, Loza-Tavera H, Avudainayagam S. 2005. Chromium toxicity in plants. Environ. Int. 31:739–753. doi:10.1016/j.envint.2005.02.003.

She FH, Tung KL, Kong LX. 2008. Calculation of effective pore diameters in porous filtration membranes with image analysis. Robot. Comput.-Integr. Manuf. 24:427–434. doi:10.1016/j.rcim.2007.02.023.

Song N, Zhong X, Li B, Li J, Wei D, Ma Y. 2014. Development of a Multi-Species Biotic Ligand Model Predicting the Toxicity of Trivalent Chromium to Barley Root Elongation in Solution Culture. PLoS ONE 9:e105174. doi:10.1371/journal.pone.0105174.

Sunda W, Huntsman S. 2003. Effect of pH, light, and temperature on Fe–EDTA chelation and Fe hydrolysis in seawater. Mar. Chem. 84:35–47. doi:10.1016/S0304-4203(03)00101-4.

Thompson SL, Manning FCR, McColl SM. 2002. Comparison of the Toxicity of Chromium III and Chromium VI to Cyanobacteria. Bull. Environ. Contam. Toxicol. 69:286–293. doi:10.1007/s00128-002-0059-9.

Tuoriniemi J, Cornelis G, Hassellöv M. 2015. A new peak recognition algorithm for detection of ultra-small nano-particles by single particle ICP-MS using rapid time resolved data acquisition on a sector-field mass spectrometer. J. Anal. At. Spectrom. 30:1723–1729. doi:10.1039/C5JA00113G.

Tuoriniemi J, Jürgens MD, Hassellöv M, Cornelis G. 2017. Size dependence of silver nanoparticle removal in a wastewater treatment plant mesocosm measured by FAST single particle ICP-MS. Environ. Sci. Nano 4:1189–1197. doi:10.1039/C6EN00650G.

Vignati DAL, Beye ML, Dominik J, Klingemann AO, Filella M, Bobrowski A, Ferrari BJ. 2008. Temporal Decrease of Trivalent Chromium Concentration in a Standardized Algal Culture Medium: Experimental Results and Implications for Toxicity Evaluation. Bull. Environ. Contam. Toxicol. 80:305–310. doi:10.1007/s00128-008-9379-8.

Vignati DAL, Dominik J, Beye ML, Pettine M, Ferrari BJD. 2010. Chromium(VI) is more toxic than chromium(III) to freshwater algae: A paradigm to revise? Ecotoxicol. Environ. Saf. 73:743–749. doi:10.1016/j.ecoenv.2010.01.011.

Viti C, Marchi E, Decorosi F, Giovannetti L. 2014. Molecular mechanisms of Cr(VI) resistance in bacteria and fungi. FEMS Microbiol. Rev. 38:633–659. doi:10.1111/1574-6976.12051.

Volland S, Lütz C, Michalke B, Lütz-Meindl U. 2012. Intracellular chromium localization and cell physiological response in the unicellular alga Micrasterias. Aquat. Toxicol. 109:59–69. doi:10.1016/j.aquatox.2011.11.013.

Figure 1.

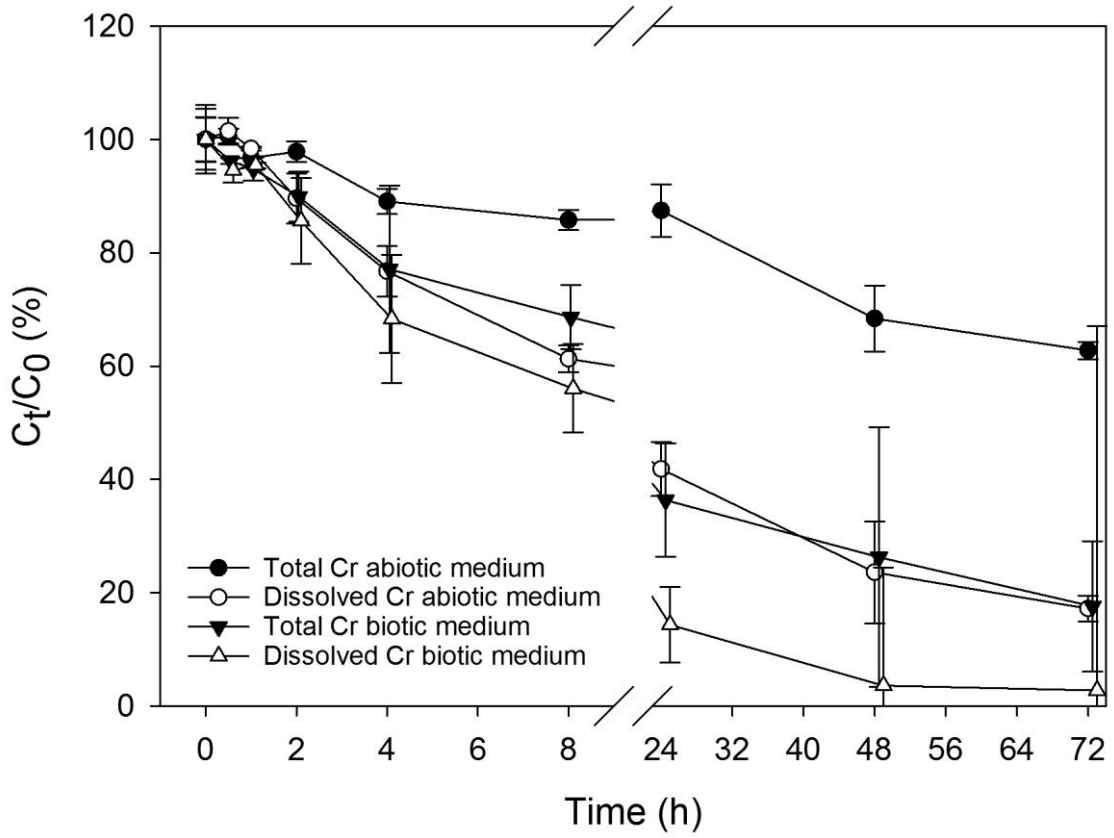

Figure 1. Temporal evolution (expressed as percentage of the value measured at t = 0) of total and dissolved (< 0.22 µm) Cr concentrations in ISO medium amended with $CrCl_3 \cdot 6H_2O$ at an initial concentration of 60 µg Cr/L (nominal value). Error bars indicate one standard deviation (SD). Large SD after 72 h of incubation were caused by Cr concentration decreasing to values close to the instrumental detection limit. C_0 and C_t refer to total or dissolved Cr concentration measured at t=0 and at the various incubation times, respectively. All data points were calculated on the basis of measured total and dissolved Cr values. The measured pH was 7.8–7.9 over the entire duration of the experiment. Data points for different incubation times were slightly nudged to visualize the corresponding error bars.

Figure 2.

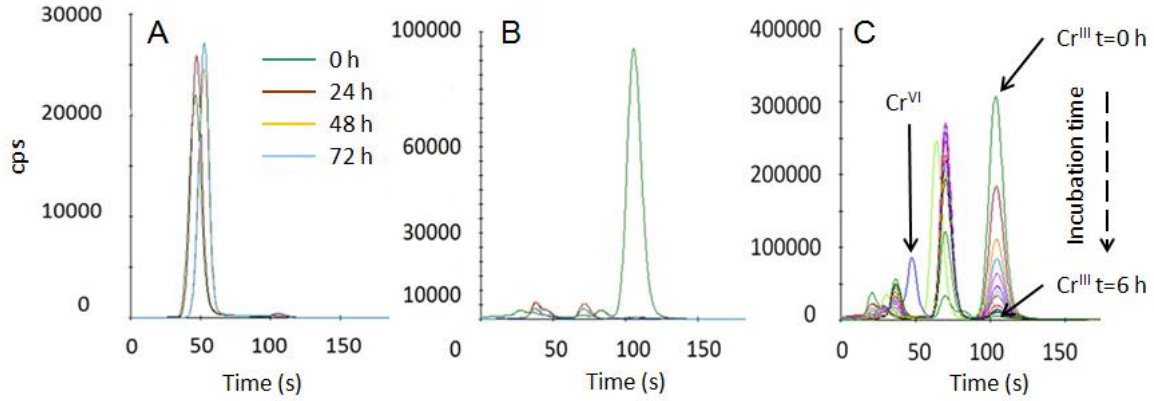

Figure 2. Chromatograms of test medium (without added algae) at different incubation times. Panels A and B: test medium amended with 115 µg/L of Cr^{VI} ($K_2Cr_2O_7$) (A) or 60 µg/L of Cr^{III} ($CrCl_3 \cdot 6H_2O$) (B) at 0 h, 24 h, 48 h or 72 h after spiking. Panel C: temporal evolution of chromatograms of test medium containing 60 µg/L of Cr^{III} with measurements performed every 20 min during 6 h. Note the peak of added Cr(VI) (5 µg/L) at 50 s. All solutions were filtered (0.22 µm) immediately before analysis; cps (counts per second). Note the different scales on the y axes.

Figure 3.

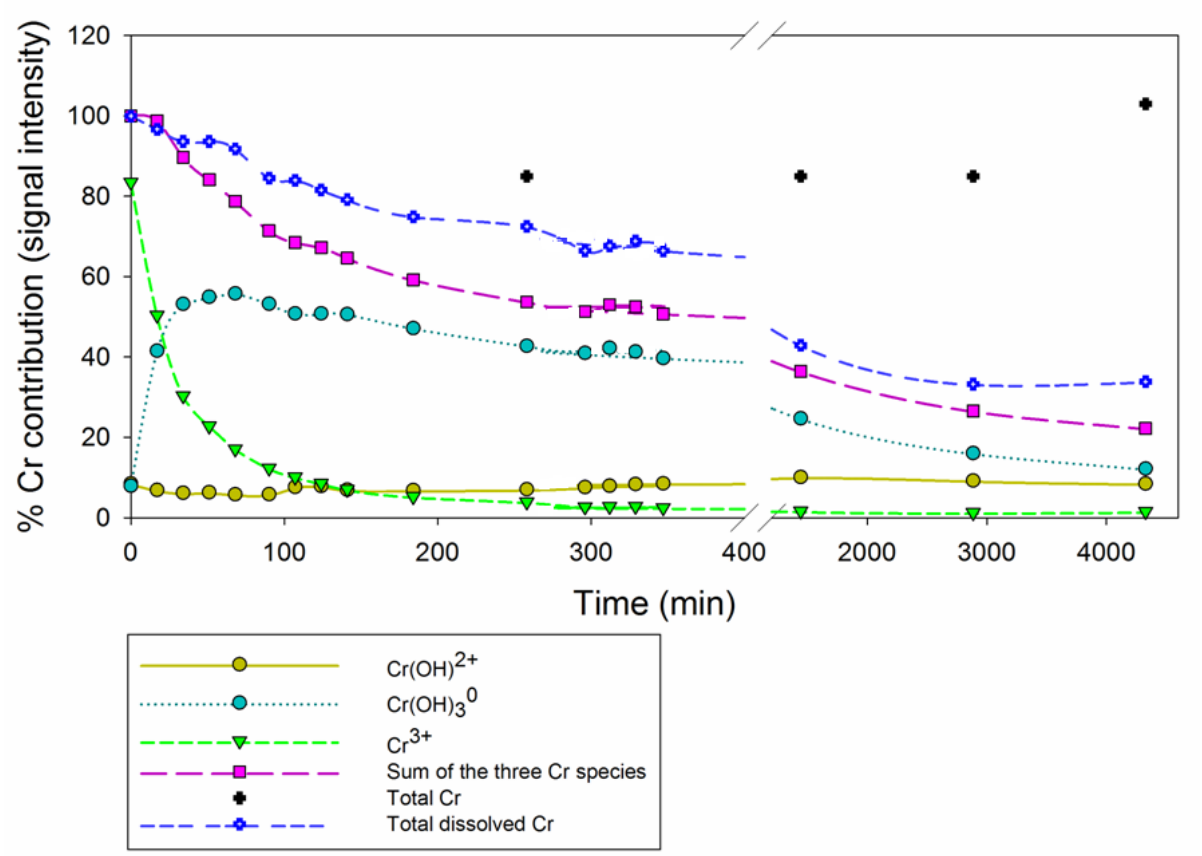

Figure 3. Temporal evolution of the relative abundances of three Cr^{III} species ($Cr(OH)^{2+}$, yellow circles; $Cr(OH)_3^0$, turquoise circles; Cr^{3+}, green triangles) in ISO medium spiked with 60 µg Cr/L of Cr^{III} ($CrCl_3 \cdot 6H_2O$) determined by IC-ICP-MS. The sum of the three Cr species (pink squares) and the signals of total chromium (black crosses) and total dissolved chromium (filtered at 0.22 µm; blue crosses) are also indicated.

Figure 4.

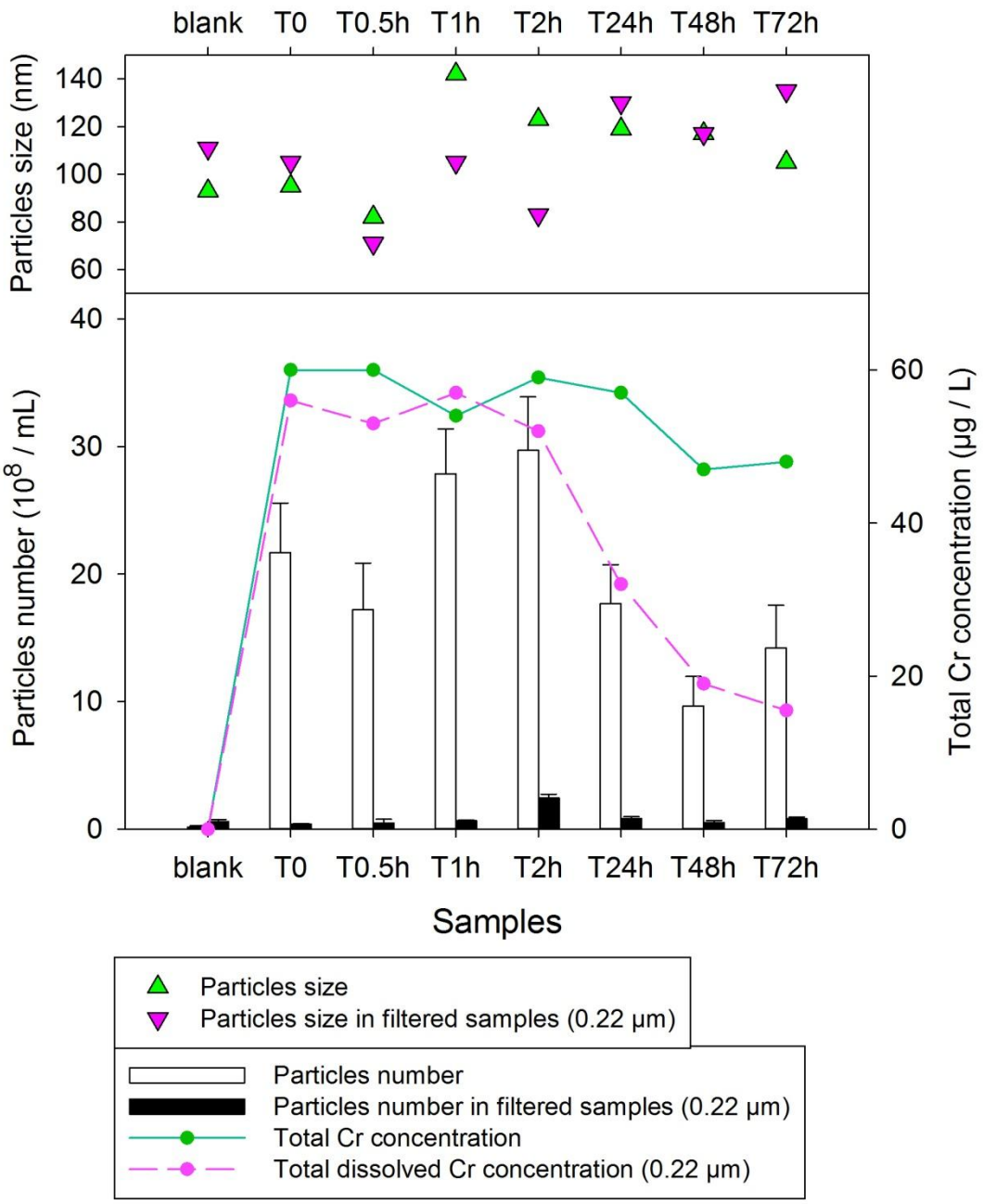

Figure 4. Particle concentrations (bars), particle size (triangles) and Cr concentration (lines) in unfiltered and filtered (0.22 µm) aliquots of ISO medium spiked (except for the sample 'Blank') with 60 µg/L of Cr^{III} ($CrCl_3 \cdot 6H_2O$) at different incubation times. Particle concentration and size measured by nanoparticle tracking analysis, Cr concentration measured by atomic absorption spectrometry.

Figure 5.

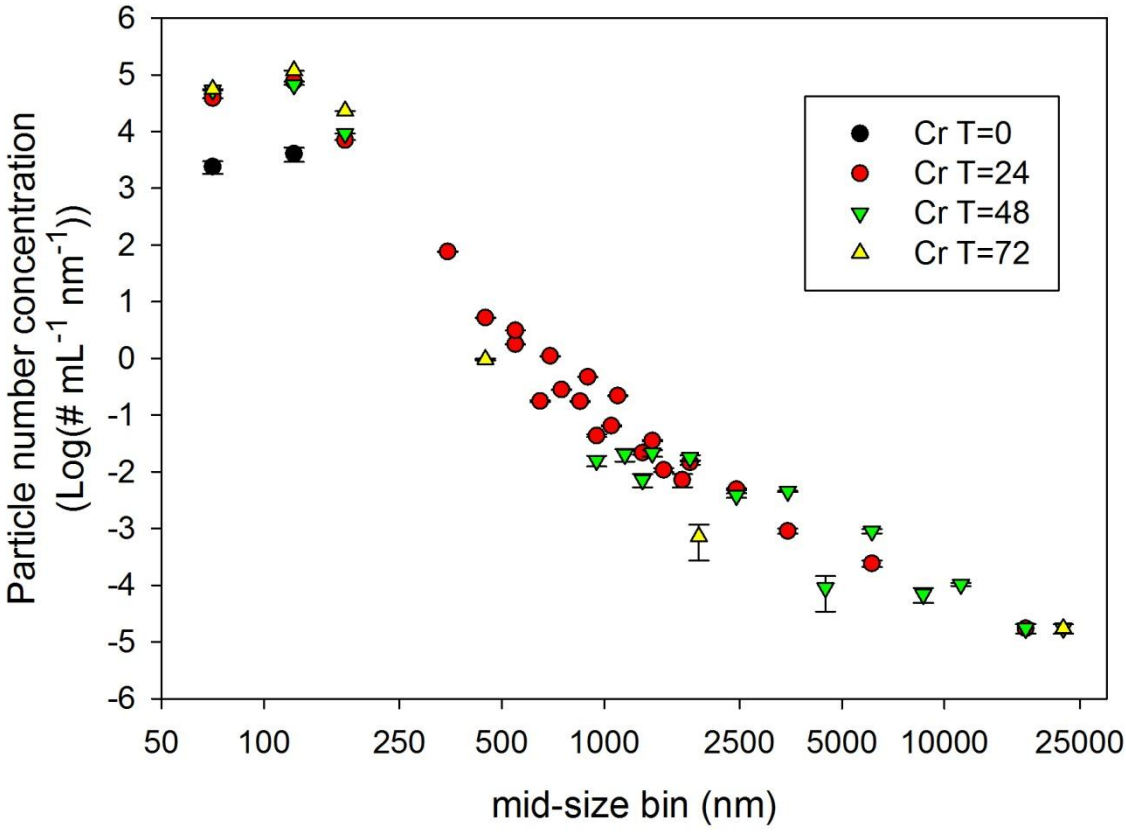

Figure 5. Particle size distribution and number of particles (in mL^{-1} nm^{-1}) in test medium spiked with Cr^{III} ($CrCl_3 \cdot 6H_2O$) after 0 (black circles), 24 (red circles), 48 (green triangles) and 72 h (yellow triangles) of incubation. All measurements were performed by Single Particle Counter (SPC) at a sample flow rate of 64 mL/min. Results for each size class have been corrected for particle concentration in ISO medium without added Cr^{III} (see figure S7 for the corresponding comparisons). To obtain the number of particles per mL in a given size range, the values on the y-axis must be multiplied for the corresponding size range (in nm) on the x-axis.

Supporting information

Chromium speciation in a standardized ecotoxicological medium: implications for hazard and risk assessment

Imad Aharchaou[a*], Jean-Sébastien Py[b], Sébastien Cambier[c], Jean-Luc Loizeau[d], Geert Cornelis[e], Philippe Rousselle[a], Eric Battaglia[a], Davide A.L. Vignati[a]

[a] Laboratoire Interdisciplinaire des Environnements Continentaux LIEC-UMR 7360, Université de Lorraine and CNRS, 8 rue du Général Delestraint, 57070 Metz, France

[b] Agence nationale de sécurité sanitaire de l'alimentation, de l'environnement et du travail ANSES-Laboratoire d'hydrologie de Nancy, 40 rue Lionnois, 54000 Nancy, France

[c] Luxembourg Institute of Science and Technology LIST, 4 avenue des hauts fourneaux-L-4362 Esch sur Alzette, Luxembourg

[d] Institute François-Alphonse Forel and Institute for Environmental Sciences, University of Geneva, 66 Bd Carl-Vogt, CH-1211 Genève, Switzerland

[e] SLU Institutionen for vatten och mijlo Lennart Hjelms väg 9, Uppsala, SE 750 07, Sweden

Twelve supplementary figures and three supplementary tables

Contents – Supporting information :

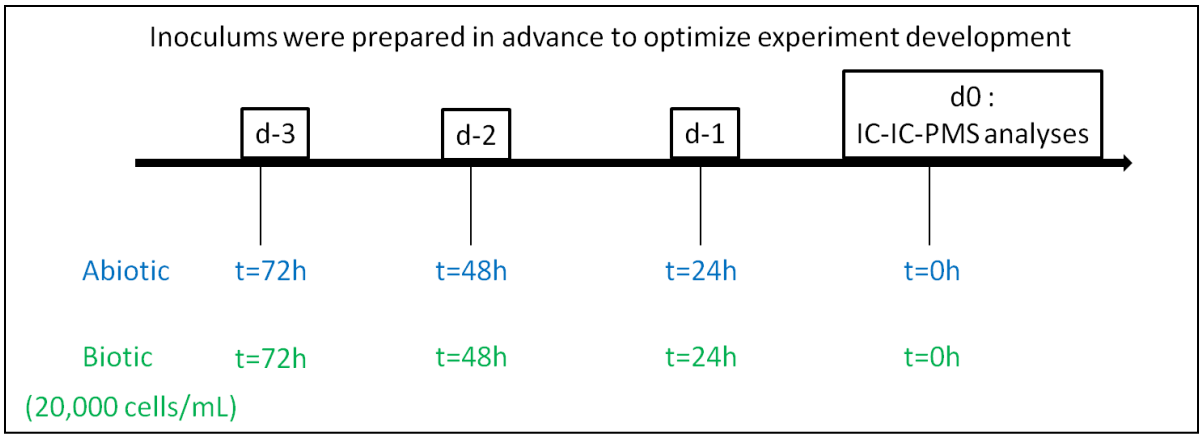

Figure S1. Experimental plan for speciation experiments with Ion Chromatography ICP-MS (IC-ICP-MS). Abiotic (absence of algae) and biotic (presence of algae) samples were prepared in advance or immediately prior to analysis (d0). All samples were analyzed on day 0 to optimize the analyses course in day 0.

Table S1: Summary of the IC-ICP-MS parameters and conditions used in Cr speciation experiments

IC conditions	
pump	Thermo ICS 5000+
separation column	Dionex Thermo AG7 2x50 mm
column temperature	20 °C
eluent	0.4 mol/L HNO_3 spiked with 1µg/L of Rh, isocratic system
flow rate	500 µL/min
sample volume	200 µL
flushing volume	1,500 µL
duration	10 min
ICP-MS parameters	
ICP-MS	Thermo XII series
nebulizer	PFA-LC
gas flow	0.87 L/min
plasma power	1,500 W
plasma gas flow	13.5 L/min
auxiliary gas flow	0.77 L/min
detector mode	pulse counting
KED	He/H_2
CCT – KED flow rate	3.5 mL/min – 3 V
Data acquisition	
ions (m/z)	^{52}Cr, ^{53}Cr, ^{103}Rh
measurement unit	counts
sweps/reading	1
replicates	1
dwell time	100 ms
integration time	600,000 ms

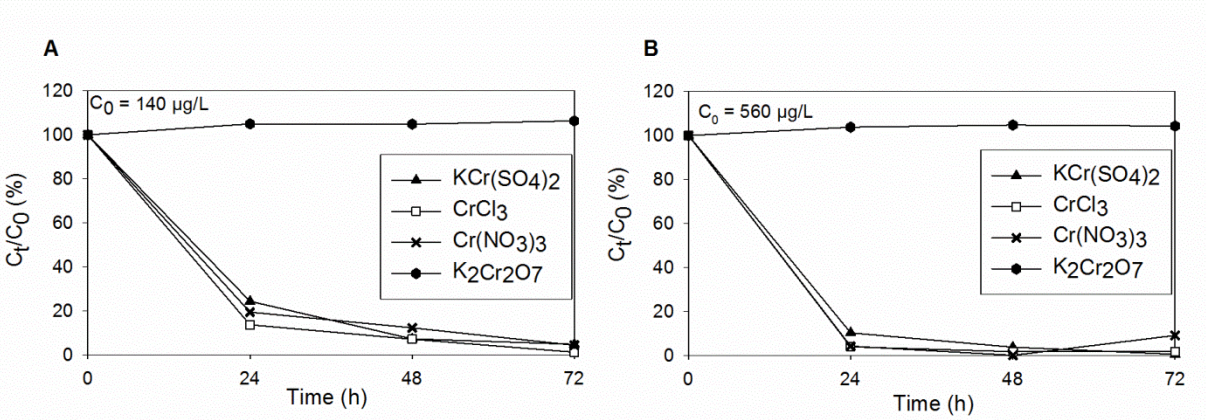

Figure S2. Temporal evolution (expressed as a percentage of the value measured at t=0) of total dissolved Cr concentrations (filtered at 0.22 µm) in standard (ISO8692) medium amended with Cr^{III} ($CrCl_3 \cdot 6H_2O$ (square) or $Cr(NO_3)_3 \cdot 9H_2O$ (cross) or $KCr(SO_4)_2 \cdot 12H_2O$ (triangle)) or Cr^{VI} ($K_2Cr_2O_7$ (circle)) during 72 hours. Initial concentration of each salt was 140 µg/L (A) or 560 µg/L (B).

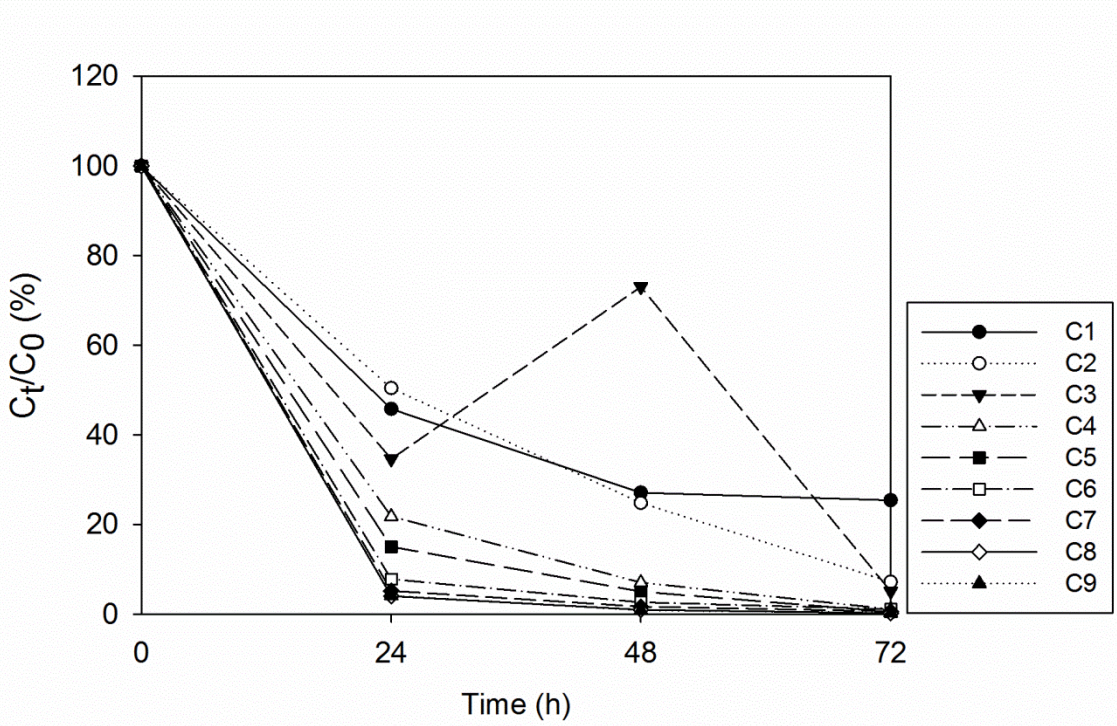

Figure S3. Temporal evolution (expressed as a percentage of the value measured at t=0) of total dissolved Cr concentrations (filtered at 0.22 µm) in standard (ISO 8692) medium amended with initial total concentrations of $CrCl_3 \cdot 6H_2O$ between 20 (C1) and 7000 (C9) µg/L (see Table S2 for the full compilation of the measured values at t = 0). Measurements were done in triplicate for C1, C2, C4 and C9 after 0 and 48 h of incubation. The relative standard deviations (RSD) for these measurements were usually below 10 % except for C1 at 48 h (RSD = 70%) and C2 at 48 h (RSD = 40%) and C3 at 48 h (RSD = 20%). The high RSD were obtained for analytical concentrations close to the instrumental quantification limit for FAAS. Also note that, with increasing concentrations, total dissolved Cr levels were lower than the corresponding total ones already at t = 0 (see Table S2).

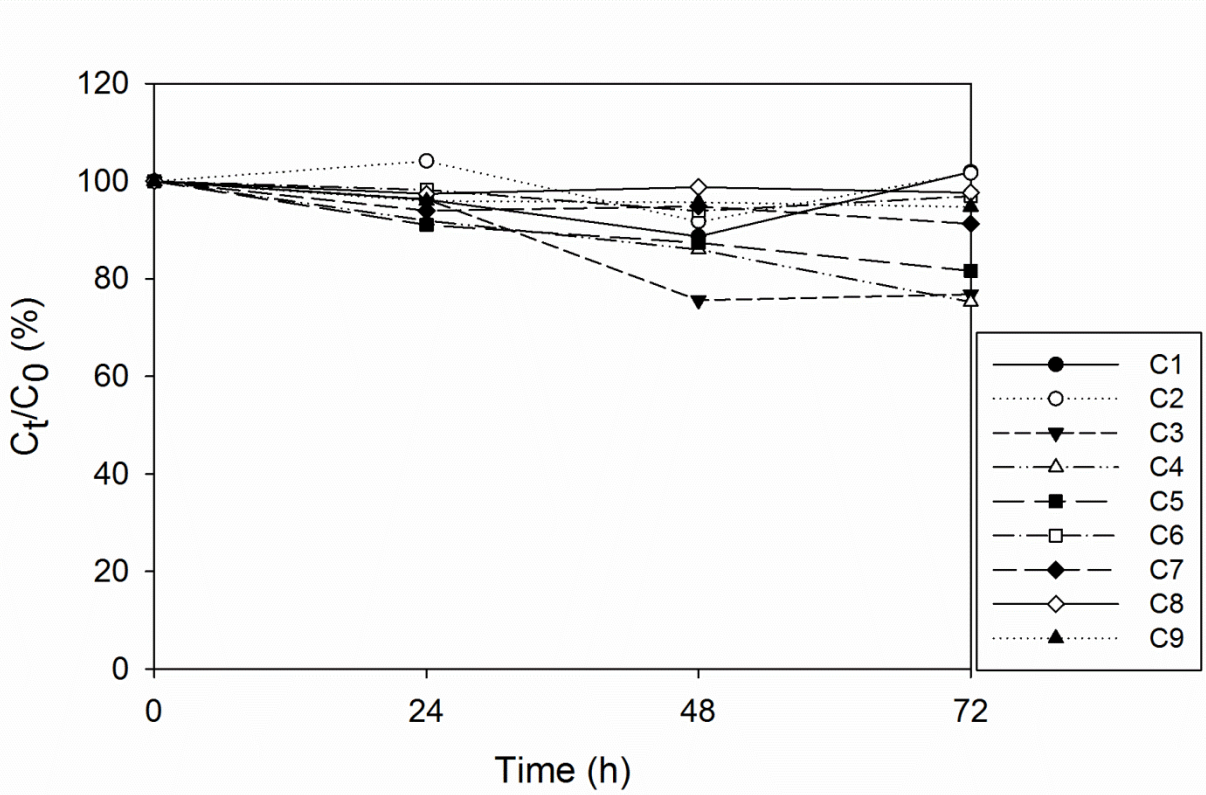

Figure S4. Temporal evolution (expressed as a percentage of the value measured at t = 0) of total Cr concentrations in standard (ISO 8692) medium amended with initial concentrations of $CrCl_3 \cdot 6H_2O$ between 20 (C1) and 7000 (C9) µg/L (see Table S2 for the full compilation of the measured values at t = 0). Measurements were done in triplicate for C1, C2, C4 and C9 after 0 and 48 h of incubation. The relative standard deviations (RSD) for these measurements were usually below 10 % except for C1 at 48 h (RSD = 20%) and C2 at 48 h (RSD = 15%).

Table S2. Measured Cr concentration at t = 0 in standard (ISO 8692) medium amended with different initial concentrations (C1–C9) of $CrCl_3 \cdot 6H_2O$ with and without filtration at 0.22 µm. All values are in µg/L of Cr.

	Measured total concentration at t = 0	Measured filterable (0.22 µm) concentration at t = 0
C1	18	20
C2	40	42
C3	82	78
C4	186	179
C5	436	379
C6	789	717
C7	1745	1477
C8	3596	2700
C9	6877	5489

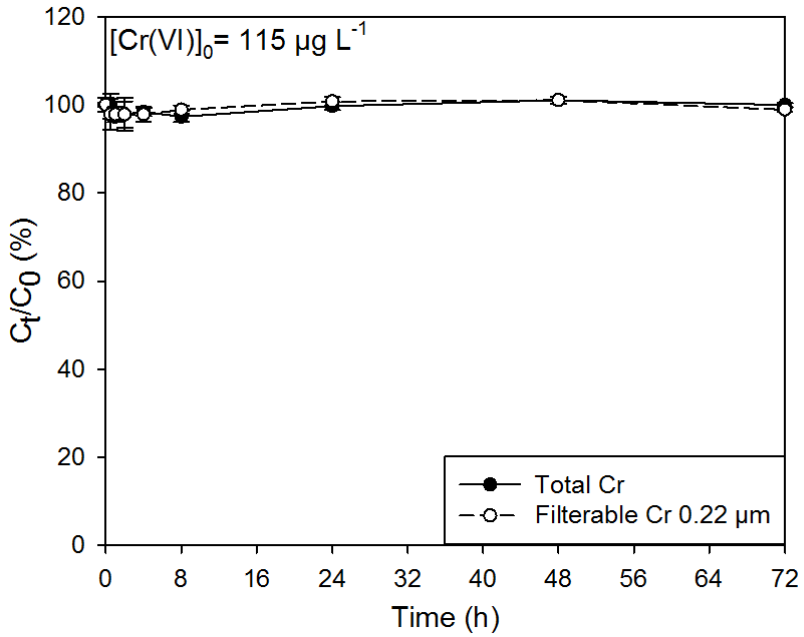

Figure S5. Temporal evolution (expressed as a percentage of the values measured at t = 0) of Cr concentrations (total Cr concentrations (black circles) and total dissolved Cr concentrations (filtered at 0.22 µm) (white circles) in biotic (presence of algae) ISO medium amended with Cr^{VI} ($K_2Cr_2O_7$) during 72 hours. Initial Cr concentration is 115 µg/L.

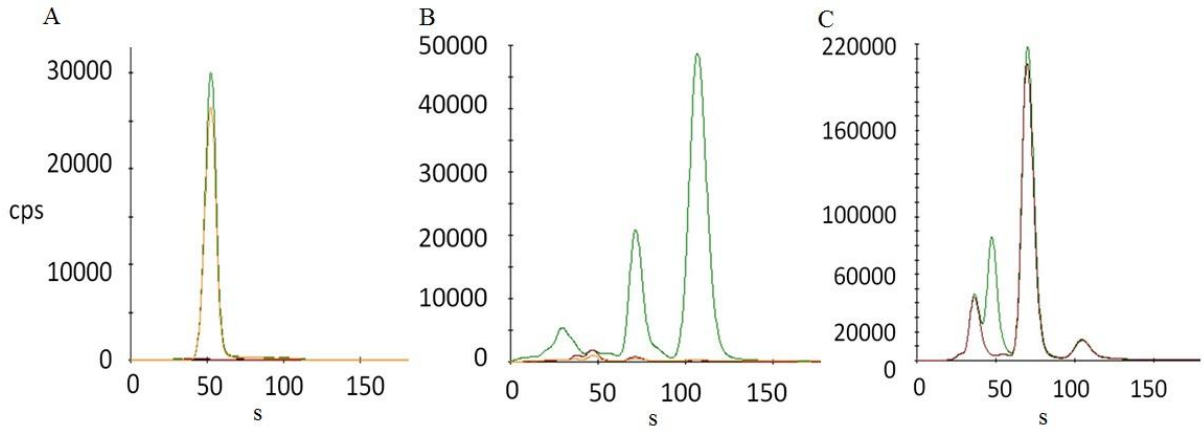

Figure S6. Chromatograms of standard ISO 8692 biotic (presence of algae, initial density ~ 20,000 cell/mL) medium amended with 115 µg/L of Cr^{VI} ($K_2Cr_2O_7$) (A) or with 60 µg/L of Cr^{III} ($CrCl_3 \cdot 6H_2O$) (B) at 0 h (green), 24 h (brown), 48 h (orange) or 72 h (blue) after spiking. Chromatograms of standard ISO 8692 medium containing 60 µg/L of Cr^{III} ($CrCl_3 \cdot 6H_2O$) during 24 h (brown), and then amended with Cr^{VI} ($K_2Cr_2O_7$) (green) (C). All solutions were filtered (0.22µm) immediately before analysis; cps (counts per second).

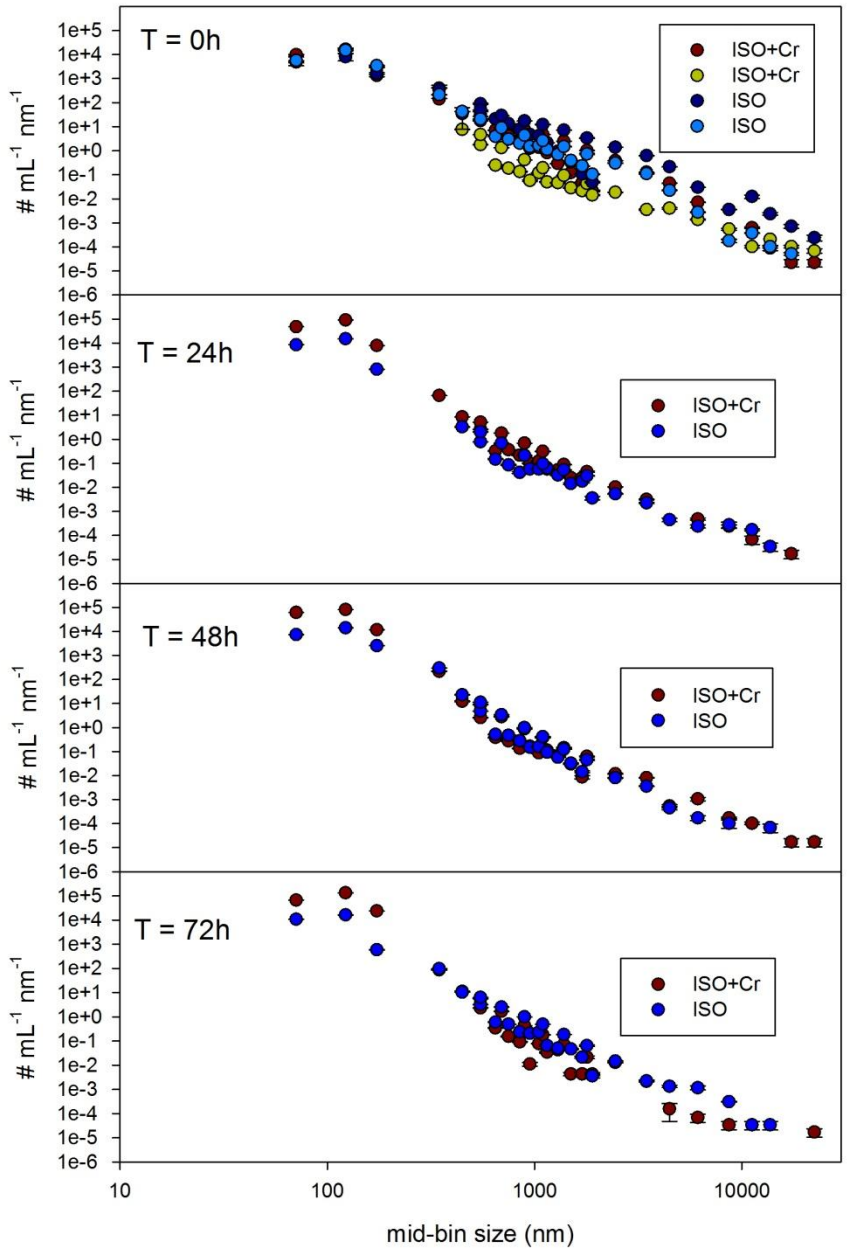

Figure S7. Particle size distribution and number of particles (in mL^{-1} nm^{-1}) determined with Single Particle Counter (SPC) measurements in ISO algal test medium with and without addition of 70 µg/L of Cr^{III} (added as $CrCl_3.6H_2O$) at different incubation times. To obtain the number of particles per mL in a given size range, the values on the y-axis must be multiplied for the corresponding average size value (in nm) on the x-axis.

Optimization of operating conditions for Nanoparticle Tracking Analysis with Nanosight NS500 instrument (Malvern instruments Ltd, UK)

In a preliminary experiment, aliquots of test medium spiked with 0, 17, 35, 70, 140 and 280 µg/L, partly covering the concentration range used in toxicity test, were analyzed by NTA. No particles were observed in aliquots spiked with 17 µg/L Cr^{III} and too many particles were detected in aliquots spiked with 140 µg/L and 280 µg/L Cr^{III}. Particle concentrations in the range $1–3\times10^9$ particles/mL were observed in solutions containing 35 and 70 µg/L Cr^{III}. The latter concentration, closed to the observed 72h EC50 for Cr^{III}, was chosen for detailed analysis after 1, 15, 30, 45, 60, 90 and 120 min, and 24, 48 and 72 h of incubation.

No particles were detected in the ultrapure water (MQW) used to prepare the test medium. Particle concentration in the blank sample (freshly prepared ISO medium) was low ($0.14 \pm 0.07 \times 10^8$ particles/mL) and particle size distribution (PSD) covered a large spectrum between 0 and 900 nm (Figure S9). In ISO medium spiked with Cr^{III} and regardless of the incubation time, particle concentrations ranged between 7.85×10^8 and 27.5×10^8 particles/mL with relative standard deviations (RSD) between 6 and 59 % (Figure S8 and S9). Particles detected by NTA had a mean size between 100 and 135 nm with RSD between 1% and 12% (Figure S9). The high RSD of some particle concentration measurements were caused by the systematic decrease in particle number between the first and the third replicate measurement (Figure S9 A, B and C). The total (unfiltered) Cr concentration was stable over 72 h and ranged between 62 µg/L at t=0 and 66 µg/L 72 h after spiking. However, the total filterable Cr concentration decreased over time from 60 µg/L at t=0 to 16 µg/L after 72 h (Figure S10). Examination of the videos recorded during NTA showed that the number of particles visible in the field of the camera was stable during data acquisition for the first replicate, but increased with time for replicates two and three.

Measurement parameters were modified by adding a waiting step of 60 s before data acquisition for replicates two and three and RSD on particle concentrations was reduced to 1–11% (Figure S9 D, E and F).

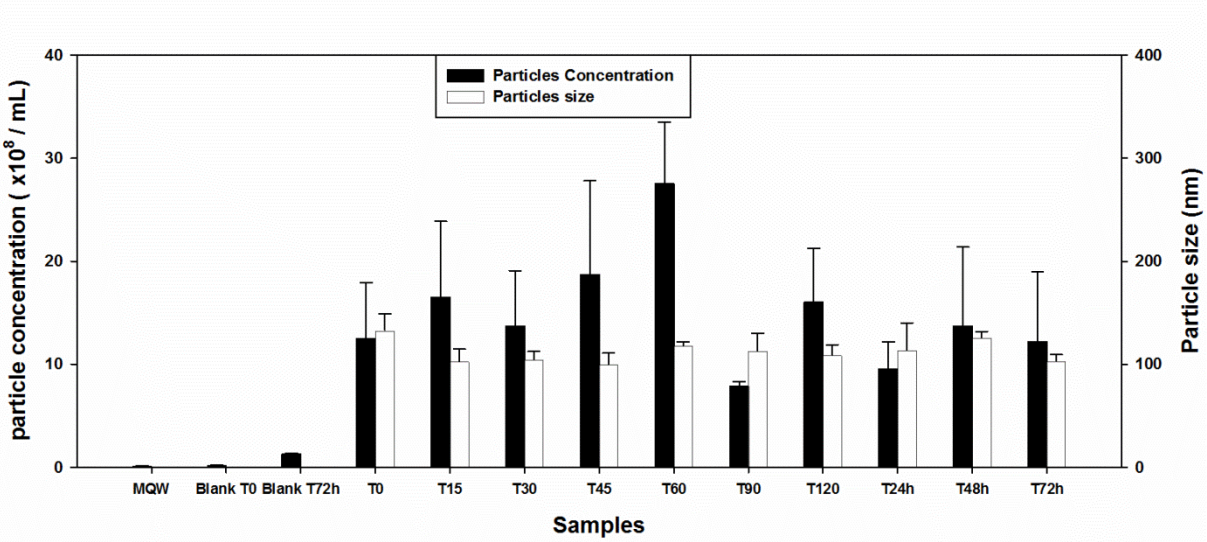

Figure S8. Particle concentration (black bars) and size (white bars) measured by nanoparticles tracking analysis (NTA) in standard (ISO 8692) medium spiked or not with 70 µg/L of $CrCl_3 \cdot 6H_2O$ for different incubation time between 0 and 120 min and after 24, 48 and 72 h.

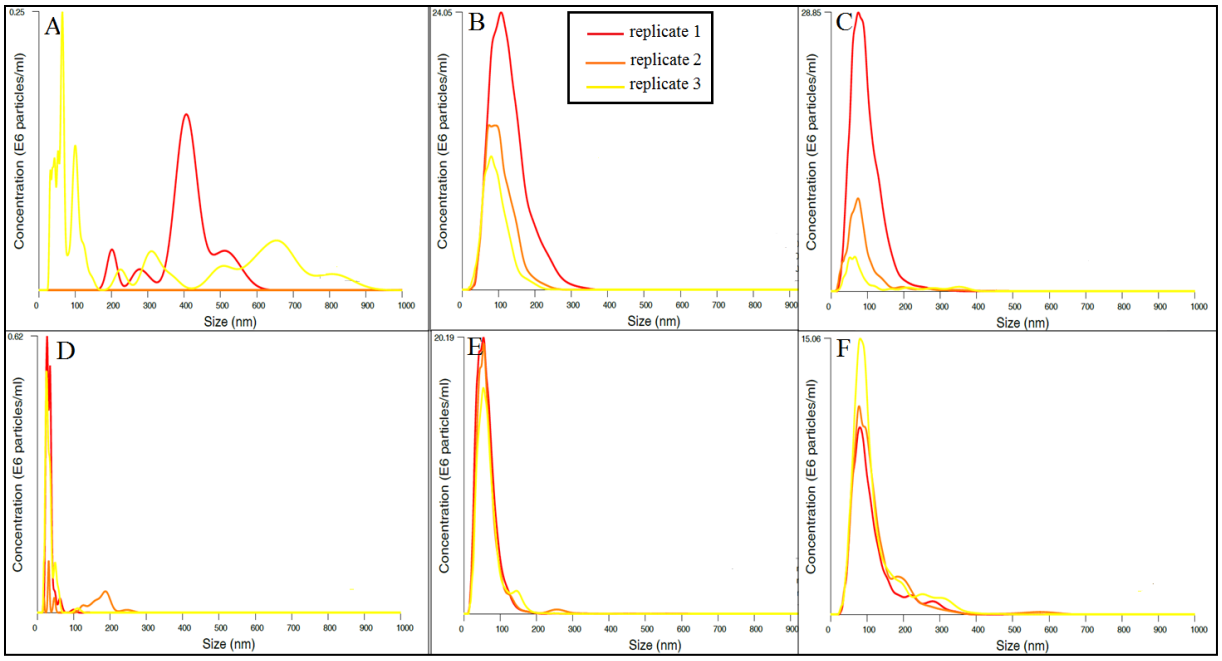

Figure S9. Comparison of reproducibility of results profiles before (A, B and C) and after (D, E and F) measurement parameters modification by adding a waiting step of 60 s before data acquisition for replicates 2 and 3. This edit to the experimental procedure aimed to harmonize the waiting time before each replicate measurement; i.e. to increase the waiting time for replicates two and three from 5 seconds to 60 s. This experiment was realized in ISO test medium spiked with 60 µg/L of Cr^{III}, corresponding to the previously determined EC50 at 72 h

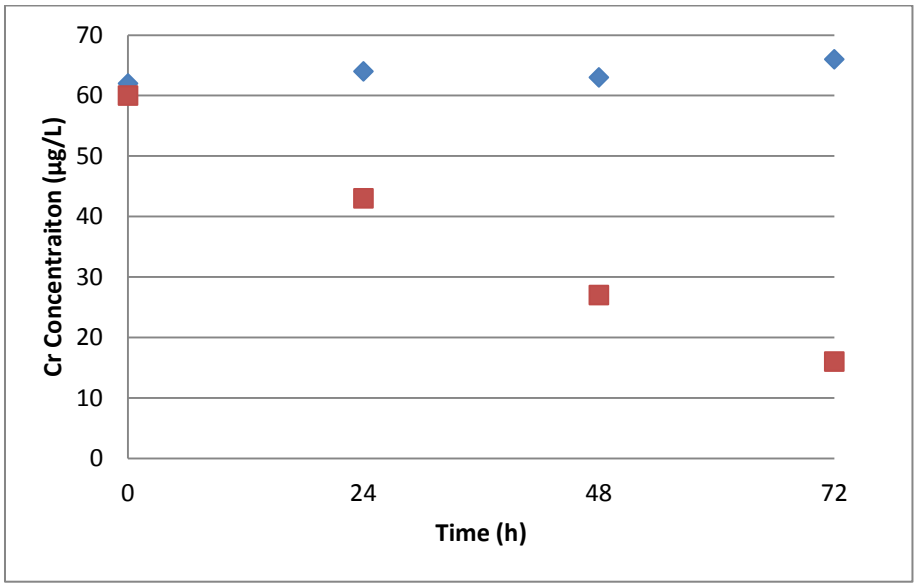

Figure S10. Temporal evolution of Cr concentrations in µg/L (total Cr concentrations (blue squares), and filterable Cr concentrations (0.22 µm) (red squares) in ISO medium amended with Cr^{III} ($CrCl_3.6H_2O$) during 72 hours. Initial nominal Cr concentration is 70 µg/L.

Corresponding spherical size and number concentration determination using single particle ICP-MS (spICP-MS) analysis using the Nexion 350 D

When nanoparticles arrive in the ICP-MS plasma they are turned into ions thus forming a cloud of ions. Truly dissolved ions are homogeneously distributed in solution and when injected into the plasma thus cause a continuous, yet fluctuating, stream of ions to be detected by the detector. Nanoparticles can thus be distinguished from dissolved ions as the former cause intensive peaks in the detected time dependent signal, each time a cloud of ions from a nanoparticle arrives at the detector. The intensity of this peak can be calculated into some measure of size, provided that a composition and shape are assumed for the particles (Table S3). Only one isotope (^{52}Cr) was measured simultaneously, whereas any Cr-containing particles formed because of hydrolysis most likely also contained oxygen atoms and protons.

No collision cell gas was used to remove $^{40}Ar^{12}C$ interferences on the ^{52}Cr signal. Hence, a continuous background signal was recorded, not consisting of ^{52}Cr but of the $^{40}Ar^{12}C$ interference. However, by using short dwell times, the intensity of any background signal reduces proportionally more than the short but intense nanoparticle signals [1]. It was thus hypothesized that better size detection limits could be obtained by using a relatively small dwell time, but still measuring in standard mode, where the sensitivity towards the most abundant Cr isotope (^{52}Cr) is highest. The used dwell time of 50 µs and the absence of settling time cause nanoparticle events to be spread over multiple subsequent measurement events that need to be integrated separately for each event. Moreover, distinguishing non-dissolved from dissolved signals was needed, because interferences still caused a relatively high background signal. Both requirements were achieved using a previously published method [2]. This method calculates an intensity cut-off value based on a number of times the standard deviation of the background signal. Integrated peak surfaces below this cut-off value are considered to stem from dissolved events and are not taken into account when recalculating

the average signal and the standard deviation of the background signal. The method converges when no new particle events are identified and the particle size distribution is then calculated from the particle events intensities. Such a single cut-off value is known to lead to both false positives (peaks mistakenly considered particle events) and false negatives (peaks mistakenly considered dissolved events) [3]. The goal of the spICP-MS measurement was to verify the hypothesis of the presence of Cr-containing particles in the samples. Hence, a high and thus conservative number of standard deviations (5) was used to minimize false positives, rather than to minimize false negatives [4].

The calculations were realized with a software called Nanocount, which is freely available at http://blogg.slu.se/Nanocount.

1211 Table S3: Conditions and ICP-MS parameters for spICP-MS analysis

ICP-MS parameters	
ICP-MS	Nexion 350D
nebulizer	GE Micromist
gas flow	0.87 L/min
plasma power	1,500 W
plasma gas flow	13.5 L/min
auxiliary gas flow	0.77 L/min
detector mode	pulse counting
KED	Standard
Data acquisition	
ions (m/z)	^{52}Cr
measurement unit	counts
sweeps/reading	10^6
replicates	1
dwell time	0.05 ms
integration time	50,000 ms
Data treatment	
Integration method	Fixed window
Peak integration time	20 ms
Minimum cluster size	4 ions
Signal discrimination method	Outlier analysis
Number of standard deviations for cut-off calculation	5
Assumed composition	$Cr(OH)_3$
Assumed density	3.11 g cm^{-3}
Assumed shape	sphere

1212

1213

1214

1215

1216

1217

1218

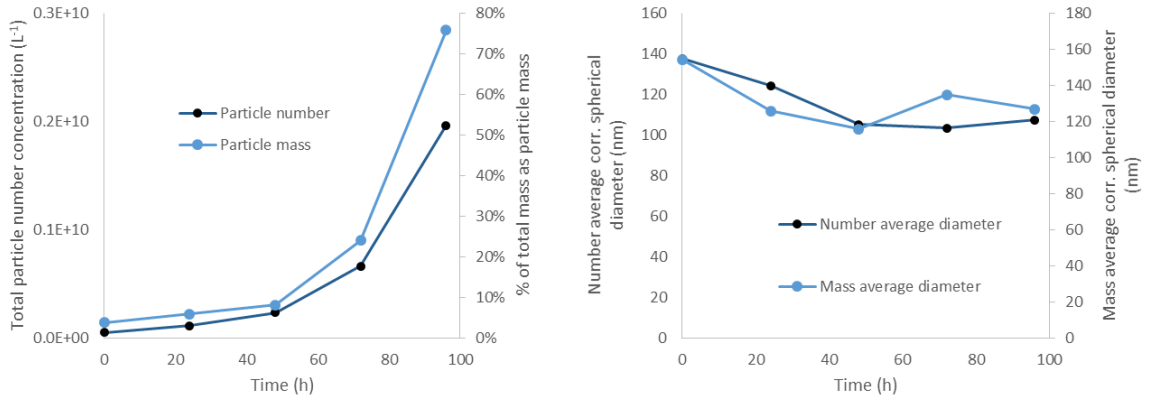

Figure S11. Temporal evolution of particle number and % of total mass occurring as particle mass (left) or number average and mass average particle diameter (right). The diameters are corresponding spherical diameters calculated using the setting in Table S3.

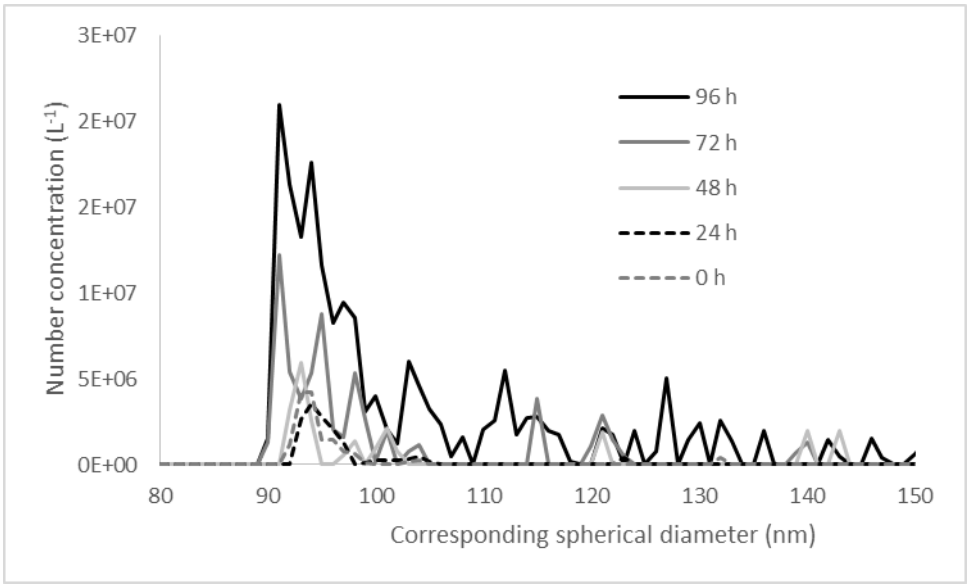

Figure S12. Temporal evolution in the distribution of the corresponding spherical diameter. The diameters are corresponding to spherical diameters calculated using the setting in Table S3.

References

(1) Montaño MD, Badiei HR, Bazargan S, Ranville JF.2014. Improvements in the detection and characterization of engineered nanoparticles using spICP-MS with microsecond dwell times. *Environ. Sci. Nano*. 1(4): 338–346.

(2) Tuoriniemi J, Cornelis G, Hassellöv MA.2015. new peak recognition algorithm for detection of ultra-small nano-particles by single particle ICP-MS using rapid time resolved data acquisition on a sector-field mass spectrometer. *J. Anal. At. Spectrom. 30* (8): 1723–1729.

(3) Cornelis G, Hassellöv MA.2013. signal deconvolution method to discriminate smaller nanoparticles in single particle ICP-MS. *J. Anal. At. Spectrom. 29* (1): 134–144.

(4) Tuoriniemi J, Cornelis G, Hassellöv M. 2012. Size Discrimination and Detection Capabilities of Single-Particle ICPMS for Environmental Analysis of Silver Nanoparticles. *Anal. Chem. 84* (9): 3965–3972.